

Spring 2015

Measurement Of Multidirectional Thermal Conductivity Of Im7-G/ 8552 Unidirectional Composite Laminate

Furkan Ismail Ulu

North Carolina Agricultural and Technical State University

Follow this and additional works at: <https://digital.library.ncat.edu/theses>

Recommended Citation

Ulu, Furkan Ismail, "Measurement Of Multidirectional Thermal Conductivity Of Im7-G/8552 Unidirectional Composite Laminate" (2015). *Theses*. 264.
<https://digital.library.ncat.edu/theses/264>

This Thesis is brought to you for free and open access by the Electronic Theses and Dissertations at Aggie Digital Collections and Scholarship. It has been accepted for inclusion in Theses by an authorized administrator of Aggie Digital Collections and Scholarship. For more information, please contact iyanna@ncat.edu.

Measurement of Multidirectional Thermal Conductivity of IM7-G/8552 Unidirectional
Composite Laminate

Furkan Ismail Ulu

North Carolina A&T State University

A thesis submitted to the graduate faculty
in partial fulfillment of the requirements for the degree of

MASTER OF SCIENCE

Department: Mechanical Engineering

Major: Mechanical Engineering

Major Professor: Dr. Kunigal Shivakumar

Greensboro, North Carolina

2015

The Graduate School
North Carolina Agricultural and Technical State University

This is to certify that the Master's Thesis of

Furkan Ismail Ulu

has met the thesis requirements of
North Carolina Agricultural and Technical State University

Greensboro, North Carolina
2015

Approved by:

Dr. Kunigal Shivakumar
Major Professor

Dr. Dhananjay Kumar
Committee Member

Dr. Frederick Ferguson
Committee Member

Dr. Samuel Owusu-Ofori
Department Chair

Dr. Sanjiv Sarin
Dean, The Graduate School

Biographical Sketch

Furkan Ismail Ulu was born on April 6th, 1988 in Istanbul, Turkey. His hometown is Istanbul, Turkey. He finished his elementary and high school education in Istanbul. His father encouraged him to pursue a degree in Engineering because his success in mechanical engineering industries. He earned his Bachelor of Science degree in Mechanical Engineering from Sakarya University in 2010 and went on to gain Master of Science degree in Mechanical Engineering. He is currently a candidate for the Masters of Science degree in Mechanical Engineering and interested in pursuing a Ph.D. in same field.

Acknowledgments

I would like to express my most sincere appreciation to my advisor Dr. Kunigal Shivakumar for his encouragement and pushing me to do my best in my research. I would like to thank Dr. Messiha Saad for initiating this research. I wish to extend my thanks to my thesis committee members, Dr. Dhananjay Kumar and Dr. Frederick Ferguson for their reviewing and assistance to move my thesis forward.

A special thanks to the staff and faculty of Center of Composite Materials Research (CCMR) and Department of Mechanical Engineering for their support during my research. Special thanks to Mr. Matthew Sharpe, Composite Materials Lab Manager, for his help in fabricating composite laminate, preparation of the test specimens and testing.

I also would like to acknowledge the support of other staff Dr. Raghu Panduranga and Mr. John Skujins for their encouragement and guidance. I would like to thank former and current students of CCMR: Ali Osman, Kazi Imran, Sidharth Karnati, Torrence Marunda, Hiba Ahmed, Russell Smyre, and Zadok Abrahaim.

Table of Contents

List of Figures	ix
List of Tables	xii
Abstract	1
CHAPTER 1 Introduction.....	2
1.1 Background of Fiber Reinforced Composites	2
1.2 Literature on Thermal Properties and Thermal Conductivity Measurement.....	4
1.2.1 Experimental approaches.....	4
1.2.2 Micromechanics models.....	6
1.2.2.1 Rule of mixture for axial thermal conductivity (k_1).....	6
1.2.2.2 Models for transverse thermal conductivity (k_3).....	7
1.3 Composite Material of Interest	9
1.4 Objective of the Research.....	10
1.5 Scope of the Thesis	10
CHAPTER 2 Experimental Approach	11
2.1 Introduction.....	11
2.2 Approach.....	11
2.3 Measurement of Thermal Diffusivity	12
2.3.1 Flash method mathematical model.....	12
2.3.2 Flashline apparatus	14
2.3.3 Experimental procedure.....	16
2.3.4 Calculation and correction.....	17
2.4 Measurement of Specific Heat Capacity	18
2.4.1 Differential Scanning Calorimetry model.....	19

2.4.2 DSC apparatus	20
2.4.3 Experimental procedure.....	22
2.5 Validation of Methodology.....	24
2.6 Preparation of Unidirectional Composite Test Samples.....	26
2.7 Summary	27
CHAPTER 3 IM7-G/8552 Carbon Epoxy Composite Materials	29
3.1 Introduction.....	29
3.2 Fabrication of Panels	29
3.3 Principal Directions of Thermal Property Measurement.....	30
3.4 Specimen Preparation	31
3.4.1 Diffusivity measurement test samples	31
3.4.2 Specific heat measurement test samples.....	33
3.4.3 Optical microscopy of specimen.	35
3.4.4 Specimens for special study	37
3.5 Summary	38
CHAPTER 4 Experiment and Results	39
4.1 Introduction.....	39
4.2 The Measurement of Thermal Diffusivity	39
4.2.1 Axial thermal diffusivity	41
4.2.2 Transverse thermal diffusivity (α_3).....	46
4.3 Measurement of Specific Heat (C_p).....	50
4.4 Thermal Conductivity	56
4.5 Special Studies	59
4.5.1 Specimen shape effect on specific heat capacity.....	59

4.5.2 Effect of surface coating on thermal diffusivity.....	63
4.6 Summary.....	65
CHAPTER 5 Thermal Conductivity of Fiber Reinforced Composites by Micromechanics.....	67
5.1 Introduction.....	67
5.2 Unit Cell Model.....	67
5.2.1 Axial conductivity (k_1) models.....	68
5.2.2 Transverse conductivity (k_3) models.	69
5.2.3 Comparison of predicted k_3 with experimental data.....	72
5.3 Summary.....	73
CHAPTER 6 Concluding Remarks and Future Work.....	74
6.1 Concluding Remarks	74
6.2 Future Work.....	76
References.....	77

List of Figures

Figure 1.1 Classification of composite materials (Daniel & Ishai, 1994)	3
Figure 1.2 Multidirectional composite laminate.....	4
Figure 2.1 Methodology of Flash Method	13
Figure 2.2 Block Diagram of a Flash System	15
Figure 2.3 Experimental Setup for the Thermal Diffusivity measurement	16
Figure 2.4 The Flash Method Thermogram.....	18
Figure 2.5 DSC 200 F3 Maia®.....	21
Figure 2.6 Cross-sectional view of DSC 200 F3 Maia®	22
Figure 2.7 Validation of Flash Method with literature data.....	25
Figure 2.8 Validation of DSC with literature data.....	26
Figure 2.9 Transverse conductivity, and diffusivity ($k_2 = k_3$), ($\alpha_2 = \alpha_3$)	27
Figure 2.10 Axial conductivity, and diffusivity (k_1), (α_1).....	27
Figure 3.1 Through the thickness direction of IM7-G/8552 unidirectional composite material ..	30
Figure 3.2 Axial direction of IM7-G/8552 unidirectional composite material.....	31
Figure 3.3 Specimen model of thermal diffusivity through the thickness (t-t-t) samples	32
Figure 3.4 Photography of thermal diffusivity through the thickness (t-t-t) samples.....	32
Figure 3.5 Specimen model of thermal diffusivity axial direction samples	32
Figure 3.6 Thermal diffusivity axial direction samples	32
Figure 3.7 Specimen geometry of specific heat samples	34
Figure 3.8 Photograph of test samples.....	34
Figure 3.9 Nikon Eclipse LV150	36

Figure 3.10 Optical image of x_1 - x_2 planes the thin specimen for transverse diffusivity measurement in x20 magnification	37
Figure 3.11 Optical images of x_2 - x_3 plane of the thick samples for axial diffusivity measurement in x50 magnification	37
Figure 3.12 Square Shape Samples Figure 3.13 Rectangular Shape Samples	38
Figure 4.1 The FlashLine™ 2000	40
Figure 4.2 The FlashLine™ 2000 specimen holders and specimens.....	41
Figure 4.3 Axial thermal diffusivity diagram of IM7-G/8552(5 Samples)	44
Figure 4.4 Error diagram of axial thermal diffusivity test.....	46
Figure 4.5 Transverse thermal diffusivity of IM7-G/8552(4 Samples).....	49
Figure 4.6 Error Bars of transverse thermal diffusivity measurement.....	50
Figure 4.7 Pans and the inside of the DSC Device	51
Figure 4.8 The Sapphire and IM7-G/8552 with pans and lids.....	52
Figure 4.9 The specific heat measurement of the IM7-G/8552	54
Figure 4.10 Error diagram of the specific heat C_p of IM7/8552	55
Figure 4.11 Thermal Conductivity of IM7-G/8552 in longitudinal direction	58
Figure 4.12 Thermal Conductivity of IM7-G/8552 in transverse direction.....	59
Figure 4.13 Specific Heat capacity versus temperature for three of different shapes of specimens	63
Figure 4.14 Thermal Diffusivity comparison of carbon coated and uncoated materials in axial direction	64
Figure 4.15 Thermal Diffusivity comparison of carbon coated and uncoated materials in transverse direction	65

Figure 5.1 Unit cell of a unidirectional composite laminate.....	67
--	----

List of Tables

Table 1.1 Properties of IM7-G fiber and 8552 matrix	9
Table 2.1 Technical Specifications of the FlashLine TM 2000 Thermal Properties Analyzer	15
Table 2.2 Technical Specifications of NETZSCH DSC 200 F3 Maia	24
Table 3.1 Physical properties of specimens	33
Table 3.2 Physical Specifications of Specimens.....	34
Table 3.3 Polishing sequence, parameters and materials (Buehler Equipment Components).....	35
Table 3.4 Physical Properties of Special Assessment Specimens	38
Table 4.1 The half time and axial thermal diffusivity values of sample 1 and sample 2	41
Table 4.2 The half time and axial thermal diffusivity values of sample 3 and sample 4	42
Table 4.3 The half time and axial thermal diffusivity values of sample 5.....	43
Table 4.4 Summary axial thermal diffusivity and average values of IM7-G/8552	43
Table 4.5 Percent error of thermal diffusivity in axial direction	45
Table 4.6 Transverse thermal diffusivity data of sample 1 and sample 2 of IM7-G/8552	47
Table 4.7 Transverse thermal diffusivity data of sample 3 and sample 4 of IM7-G/8552	47
Table 4.8 Transverse thermal diffusivity and average data of IM7-G/8552.....	48
Table 4.9 Percent error of thermal diffusivity in transverse direction	49
Table 4.10 The measured specific heat data of IM7-G/8552.....	53
Table 4.11 The Percent Error of Specific Heat Capacity.....	55
Table 4.12 Thermal Conductivity of IM7-G/8552 in axial direction, k_1	57
Table 4.13 Thermal Conductivity of IM7-G/8552 in transverse direction, k_3	57
Table 4.14 Specific heat capacity of IM7-G/8552-1 square shape samples	60
Table 4.15 Specific heat capacity of IM7-G/8552-1 circular shape samples	61

Table 4.16 Specific heat capacity of IM7-G/8552-1 rectangular shape samples	61
Table 4.17 Comparison of specific heat capacity of IM7-G/8552-1 samples	62
Table 4.18 Thermal diffusivity comparison of coated and plain samples in two directions	64
Table 5.1 Constituent thermal conductivity	68
Table 5.2 Comparison of predicted k_3 of AS Graphite/Epoxy composite with the literature data	71
Table 5.3 Comparison of predicted and measured conductivity k_3 of IM7-G/8552.....	72

Abstract

Thermal characterization of composite materials plays an important role in engineering design of thermal structures and aerospace systems and automotive, etc. There are limited data on these materials in the literature. In particular, multidirectional thermal characterization needs to be established for polymer matrix composites to determine their working temperatures and thermal conductivities. In unidirectional fiber reinforced composites, thermal conductivities are different in axial and transverse directions of the composite material. The purpose of this research was to determine multidirectional thermal conductivities of IM7-G/8552 unidirectional carbon/epoxy composite laminate and validate the data with micromechanics models and data in the literature for similar materials. IM7-G/8552 unidirectional composite material was fabricated, and two different types of specimens in axial and transverse direction were prepared. Flash Method was used to measure the thermal diffusivity in axial and transverse directions of fiber using the ASTM E-1461 standard. Differential Scanning Calorimeter was used to measure the specific heat of the composite material using the ASTM E-1269 standard. Then thermal conductivity was calculated by multiplying thermal diffusivity, specific heat capacity, and material density. The experiments were performed at temperatures ranging from 20°C to 100°C. The measured test results agreed well with micromechanics model and similar material in literature. Thermal conductivities of IM7/8552 at room temperature were $k_1 = 4.89 \text{ W/m}^\circ\text{C}$ in axial and $k_3 = 0.58 \text{ W/m}^\circ\text{C}$ in transverse directions.

CHAPTER 1

Introduction

Applications of fiber reinforced composite materials are expanding to a number of industries including transportation and infrastructure. Composite materials provide more flexibility in design of vehicles in aerospace applications. Polymer matrix fiber reinforced composite materials consist of two materials, namely, polymer matrix and reinforcing fibers. The reinforcement fiber is usually stiffer, stronger, and continuous, and the matrix phase is weaker but holds the fibers together (Daniel & Ishai, 1994). Composite materials are superior in specific strength, stiffness, fatigue, and corrosion. Because of these reasons, they are in high demand in transportation applications. Thermal properties of the materials are essential for design of thermo-mechanical structures. The thermal property such as conductivity depends on fiber direction. Furthermore, heat transfer through composite materials plays a critical role in determining thermal effect on structures. Therefore this thesis focused on measurement of thermal conductivity of IM7-G/8552 carbon composite along and across the fiber directions.

1.1 Background of Fiber Reinforced Composites

Composite materials consist of two different phases or constituents which result in superior properties than the parent constituents. These constituents are reinforcement and matrix. The reinforcement is fiber and provides stiffness and strength to the combined material. The task of matrix is to keep together the fibers in relative position to create a unique material with superior properties. Composites are classified as continuous and discontinuous fiber according to the type of reinforcement. Discontinuous-fiber composites have short fibers, whiskers or nanotubes. Continuous fibers extend along the composites. Continuous fiber reinforced composites are stronger and flexible than discontinuous fiber composites. They could be in form

of unidirectional, multidirectional or cross ply laminates. These composites can be obtained in the market as unidirectional tapes, waves or braids.

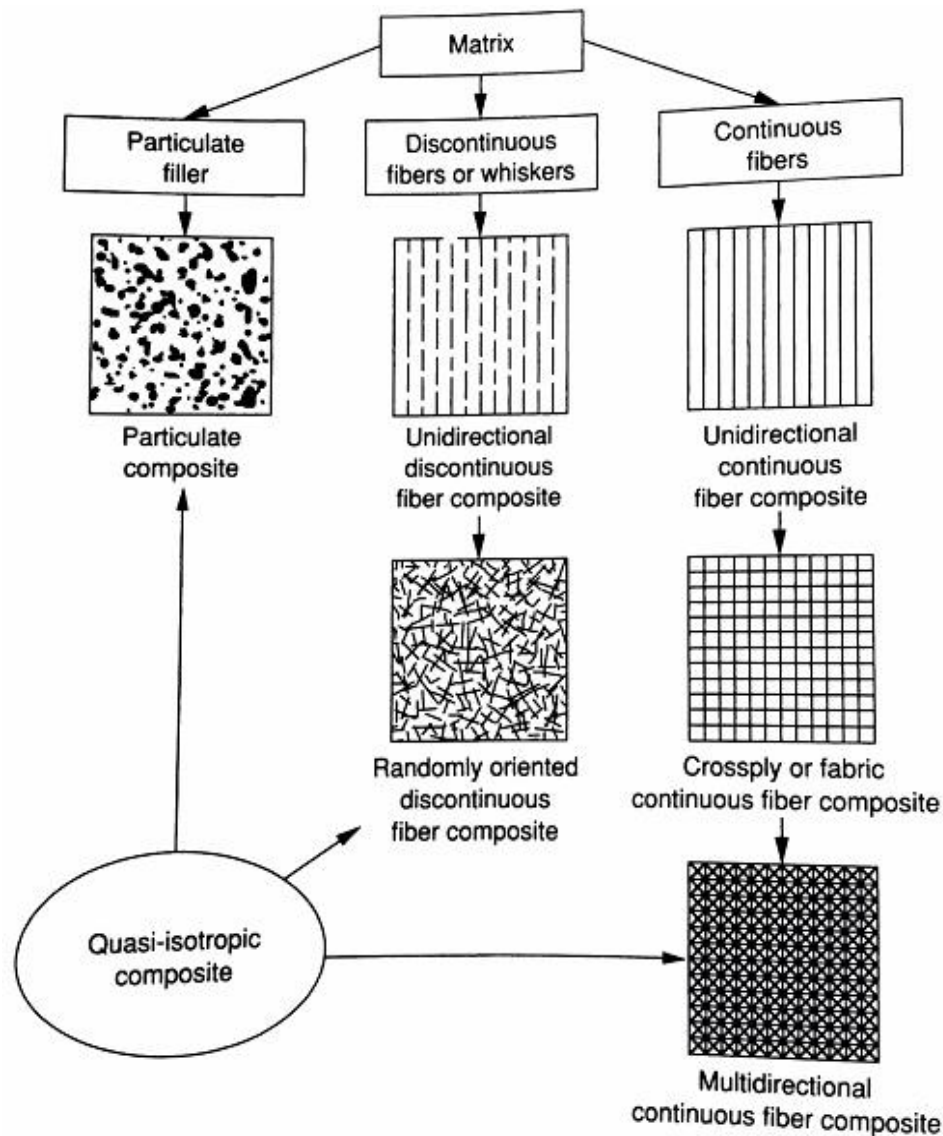


Figure 1.1 Classification of composite materials (Daniel & Ishai, 1994)

The other classification of composite materials is based on the type of matrix used. These types are polymer matrix composites (PMC), metal matrix composites (MMC), ceramic matrix composites (CMC) and carbon-carbon composites. PMC contain thermoset (epoxy, polyimide, polyester) or thermoplastic (poly-ether-ketone, polysulfone) matrix reinforced with glass, carbon

(graphite), aramid or boron fibers. Low temperature applications are usually the choice of PMC. MMC is made up metals or alloys (aluminum, magnesium, titanium, and copper) reinforced with boron, carbon or ceramic fibers. Their limitation is maximum temperature of melting points of the metal matrix. CMC consists of ceramic matrices reinforced with ceramic fibers. They are good at working at high temperature applications. Carbon-carbon composites contain carbon or graphite matrix reinforced with carbon fibers. They are superior at high temperature and thermal shock applications.

A lamina, or ply, is a layer of unidirectional fibers with a matrix. A laminate consists of two or more unidirectional lamina or plies bagged together. Laminae can be oriented in various orientations in a laminate as shown in figure 1.2. The laminate can be in form of different thicknesses and materials. The thickness is much smaller than length and width measurements.

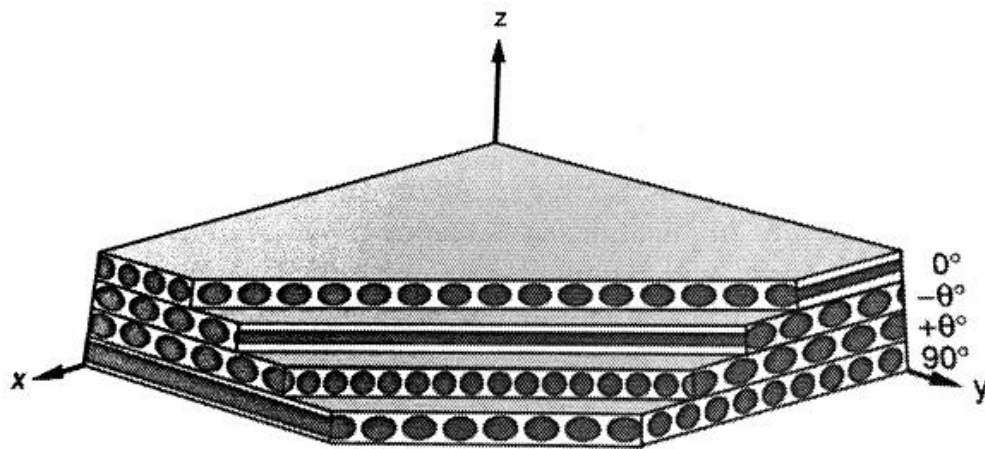


Figure 1.2 Multidirectional composite laminate

1.2 Literature on Thermal Properties and Thermal Conductivity Measurement

1.2.1 Experimental approaches. There are numbers of approaches to measure the thermal conductivity of materials. The five commonly used methods are summarized here. Steady-state method is one of the commonly used to measure the thermal conductivity. This

method cannot be performed when the temperature of the material is changing. The unknown material set up between two plates. Hot plate is placed on top and cold plate is placed below. The heat is supplied from top to down to stop convection within sample. The measurement is made after sample reach steady-state. Behzad and Sain (2007), Han et al. (2008), and Shim et al. (2002) developed the method using steady-state heat flow condition. The biggest disadvantage is that providing steady-state condition is very hard.

Transient Plane Source (TPS) is another method is used for transient temperature (changing) application. The main idea behind this technique is using a circular double nickel spiral sandwiched between thin polyimide film Kapton. The spiral is the heat source using electric power. Thermal conductivity can be calculated if variation of temperature and voltage with time, and heat flow data is known. Kalaprasad et al. (2000) and Johnston (1997) are used TPS for determination of thermal conductivities of two different materials. This method is quick however mathematical analysis of the data is in more difficult than steady-state method.

In the hot wire method, a metal is being used as heater. A pure platinum wire located between two brick. Then, a constant electric current is applied to pure platinum. Heat flows from wire into the refractory bricks. The rate of temperature increase of the platinum wire is defined by measuring the increase in the same way a platinum resistance thermometer is used (ASTM C1113, 2013). The disadvantage of this method is usually being used for isotropic materials and not a suitable for anisotropic materials.

Three- ω method (Rowe, 2005; Tian, 2011) is one of the other methods to measure the thermal conductivity. In this method, a thin narrow metal film placed on the surface with good thermal contact to the sample. The heater is driven with AC current at frequency ω which makes the heat source at frequent 2ω . Thermal conductivity can be determined by reporting AC voltage

as a function of frequency. The last voltage drop across the heating at wire 3ω has thermal properties of the material. The main difficulty to measure with this method is it needs microlithography and specialists to design the method.

Flash Laser Method is used to measure the thermal diffusivity of the material. In this method, thermal conductivity is obtained by multiplying thermal diffusivity, specific heat capacity, and density of the material. This method is simpler, accurate, and most acceptable method in the literature because of the use of commercial equipment. Flash method (commonly called) is similar to other methods of measuring thermal diffusivity: thermal wave interferometry method and thermographic method (Cernuschi et al., 2002). Since, the flash method has become the ASTM standard, it will be used in the present study.

Most of the work including the ASTM Standard here to fore was for metallic material, we use the same equipment by properly preparing test samples so that the directional diffusivity of composite is measured.

1.2.2 Micromechanics models. A number of analytical models were developed to calculate axial and transverse thermal conductivity of composites based on micromechanics analysis.

1.2.2.1 Rule of mixture for axial thermal conductivity (k_1). The resin is assumed as isotropic and the fiber is orthotropic. Determining the axial thermal conductivity of the fiber composite material can be performed by a rule of mixture. Rule of mixture is used to predict axial thermal conductivity of composites in the literature (Springer & Tsai, 1967; Thornburgh & Pears, 1965).

$$k_1 = V_f k_{1f} + V_m k_m \quad (1.1)$$

1.2.2.2 Models for transverse thermal conductivity (k_3). There are numbers of models to predict the transverse thermal conductivity in the literature. The following six models were most commonly used and accuracy of these models is validated by Wetherhold and Wang (1994), for AS Graphite/ Epoxy composite. All equations are expressed in terms of conductivities of fiber (k_3), resin (k_m) and fiber volume fraction (V_f).

1. Rayleigh (1892): Rayleigh analyzed influences of obstacles arranged in rectangular order and derived the equation for k_3 in the form:

$$k_3 \approx k_m \left(1 - \frac{2V_f}{\nu' + V_f - \frac{C_1}{\nu'} V_f^4 - \frac{C_2}{\nu'} V_f^8} \right)$$

Where;

$$C_1 = 0.3058$$

$$C_2 = 0.0134$$

(1.2)

The expression for ν' is;

$$\nu' = \frac{\left(\frac{k_m}{k_f + 1} \right)}{\left(\frac{k_m}{k_f - 1} \right)}$$

2. Halphin and Tsai (1964): Halphin – Tsai model is based on bounding principles and an analogy similar to mechanical (shear) properties:

$$k_3 = k_m \left[\frac{1 + \xi \eta V_f}{1 - \eta V_f} \right]$$

$$\eta = \frac{\left(\frac{k_f}{k_m} \right) - 1}{\left(\frac{k_f}{k_m} \right) + \xi}$$

(1.3)

Where;

When $\xi = 1$ the equation can be written as equation 1.4

3.Hashin (1983): Hashin model is based on bounding principles and analogies to mechanical (shear) properties. This model is same as Halphin-Tsai equation, except it is written in the different form:

$$k_3 = k_m + \frac{V_f}{\frac{1}{k_f - k_m} + \frac{1 - V_f}{2k_m}} \quad (1.4)$$

4.Springer and Tsai (1967): Springer – Tsai is based on simple combinations of thermal resistance model:

$$k_3 = k_m \left[\left(1 - 2\sqrt{\frac{V_f}{\pi}} \right) + \frac{1}{B} \left[\pi - \frac{4}{\sqrt{1 - \left(\frac{B^2 V_f}{\pi} \right)}} \tan^{-1} \frac{\sqrt{1 - \left(\frac{B^2 V_f}{\pi} \right)}}{1 + B\sqrt{\frac{V_f}{\pi}}} \right] \right] \quad (1.5)$$

Where; $B = 2 \left(\frac{k_m}{k_f} - 1 \right)$

5.Chawla (2012): Chawla is based on simple combinations of thermal resistance model:

$$k_3 = k_m \left(\left(1 - \sqrt{V_f} \right) + \frac{\sqrt{V_f}}{1 - \sqrt{V_f} \left(1 - \frac{k_m}{k_f} \right)} \right) \quad (1.6)$$

6.Farmer and Covert (1994): Rayleigh and Farmer-Covert models are the same except for interphasial property effect. If the interphasial effect is neglected the two models give the same results, which is the case in present analysis:

$$k_3 \approx k_m \left(1 - \frac{2V_f}{v' + V_f - \frac{C_1}{v'} V_f^4 - \frac{C_2}{v'} V_f^8} \right)$$

Where;

$$C_1 = 0.3058, \quad C_2 = 0.0134 \quad (1.7)$$

And;

$$v' = \frac{\frac{k_m}{k_f} + 1 + \frac{k_m}{ah_c}}{\frac{k_m}{k_f} - 1 + \frac{k_m}{ah_c}}$$

Here α is $3.75\mu\text{m}$ and h_c is $4 \times 10^6 \text{ W/m}^2\text{°C}$ from Wetherhold and Wang (1994) for AS Graphite/Epoxy.

1.3 Composite Material of Interest

In this study, intermediate modulus carbon fiber IM7-G and toughened 8552 epoxy composite was chosen because of wide use of the material in aircraft and rotor craft applications. Properties of IM7-G carbon fiber and 8552 epoxy are listed in table in 1.1. The IM7-G/8552 was supplied by Hexcel Corporation.

Table 1.1

Properties of IM7-G fiber and 8552 matrix

Property	IM7-G fiber	8552 matrix
Diameter, μm	4	
Density, g/cm^3	1.8	1.3
Longitudinal modulus, GPa	290	
Transverse modulus, GPa	21	
Tensile modulus, GPa		4.7
Tensile strength, MPa	5,170	120.6
Thermal conductivity, $\text{W/m}^{\circ}\text{C}$	5.4	0.1

1.4 Objective of the Research

Objective of the research is to measure axial and transverse thermal conductivity of IM7-G/8552 composite laminate as a function of temperature, verify the results with current micromechanics models. Finally, establish a simple equation as functioning temperature for IM7-G/8552 composite.

1.5 Scope of the Thesis

The thesis consists of six chapters. Chapter 1 presents the background of the research, general information about the composite laminates, literature on experimental approaches, and analytical models of thermal conductivity of composite materials. Research objectives and the scope of thesis are also in this chapter. Chapter 2 provides the experimental approach to determine the thermal conductivity of composites. Chapter 3 describes the preparation of specimens and principle directions of thermal conductivity measurement of IM7-G8552. Chapter 4 presents the results and discussion on thermal diffusivity, specific heat capacity, and thermal conductivity for IM7-G8552 composite laminate. Chapter 5 provides thermal conductivity of fiber reinforced composites by micromechanics and comparison with the experimental data. Finally, Chapter 6 presents the conclusions of the research and possible future work.

CHAPTER 2

Experimental Approach

2.1 Introduction

In this chapter, experimental approach of measuring of thermal conductivity of fiber reinforced composite material is explained. The two properties of materials are required thermal diffusivity and specific heat capacity. NETZSCH Differential Scanning Calorimeter (DSC) and Anter Flashline are used to measure specific heat and diffusivity, respectively. Mathematical principals and details of the equipment are explained. Furthermore, an approach of the conductivity measurement of unidirectional composite materials is described.

2.2 Approach

Thermal conductivity is commonly measured through thermal diffusivity, specific heat, and density. The equation to calculate thermal conductivity is shown in the following equation:

$$k = \alpha \cdot \rho \cdot C_p \quad (2.1)$$

Where α is the thermal diffusivity (m^2/s), ρ is the mass density (kg/m^3), and C_p is the specific heat capacity ($\text{J}/\text{kg}^\circ\text{C}$) of the material. Once the ρ , C_p , and α are measured, the conductivity k ($\text{W}/\text{m}^\circ\text{C}$) can be calculated. DSC and Flash method are used to determine specific heat capacity C_p and thermal diffusivity α of the materials. These methods are simple and give more reliable and accurate results than the other techniques in the literature (Cernuschi et al., 2002; Coquard & Panel, 2009). American Society for Testing and Materials Standard ASTM E-1461 (2007) describes the flash method to measure diffusivity and ASTM E-1269 (2005) DSC method to measure the specific heat.

2.3 Measurement of Thermal Diffusivity

Thermal Diffusivity is one of the significant characteristics of a material to calculate the conductivity of a material. Thermal diffusivity gives the result of how fast heat transfers through the material. There are several methods to measure thermal diffusivity. However, the flash method is used in this thesis because it is easy, reliable, and accurate and the ASTM standard is available using a commercial equipment (Cernuschi et al., 2002).

2.3.1 Flash method mathematical model. Flash Method was developed by Parker et al. (1961) and has become most common method to determine thermal diffusivity of a material. In many countries, it is considered a standard for thermal diffusivity of solid materials since flash method has no limitations on the materials (van Laack, 2014). The advantages of this method are simple specimen geometry, small specimen size requirements, and rapidity of measurement. It is defined by American Society for Testing and Materials E1461. It involves a small disc specimen is heated to desired temperature. High intensity short duration radiant energy pulse is subjected to the material when the material is reached the stated temperature. Figure 1 describes the approach of Flash Method to measure the thermal diffusivity. The energy source can be a laser or lamp. The energy is absorbed on the front surface and transfers the heat to the temperature rise (thermogram) is measured with respect to the time by IR Detector (ASTM E-1461, 2007). The data acquisition system records the change of temperature with time on the back face of the specimen.

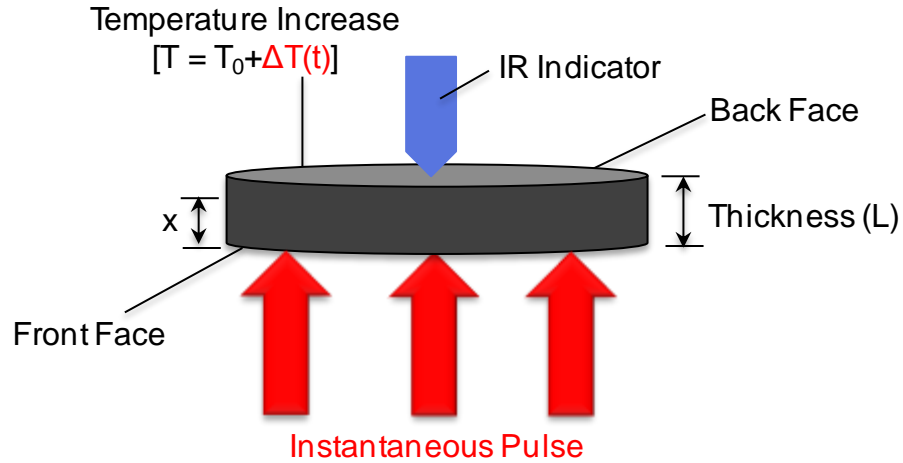


Figure 2.1 Methodology of Flash Method

After the furnace is set at specific temperature, instantaneous energy pulse is applied to the front face of the specimen. The temperature change (ΔT) with time on the back face is recorded. The energy pulse continuous until the ΔT becomes constant with respect to time. This ΔT is recorded as ΔT_{max} and the time required to reach $\frac{\Delta T_{max}}{2}$ is recorded as half time $t_{1/2}$. The half time and the specimen thickness (L in cm) are used to calculate the thermal diffusivity of the composite material in Parker's equation 2.2 (ASTM E-1461, 2007). The test is described valid if the $t_{1/2}$ resulted between 0.01 and 1 s.

$$\alpha_p = \frac{1.37 \cdot L^2}{\pi^2 t_{1/2}} \quad (2.2)$$

Parker's equation is for the ideal case and theoretical model of the flash method. Specimens are assumed isotropic and homogenous material. It assumes one dimensional heat transfer, no heat loss, and energy pulse is uniform and instantaneous. Many other researchers proposed correction factors to Parker's equation to consider the heat loss, finite pulse time, and non-uniform heating effects. Cowan, Clark and Taylor, Koski, and Heckman's correction factors are mostly used in the literature (Clark III & Taylor, 1975; Cowan, 1963; Heckman, 1973). These correction factors

can be used together to place additional parameters. The one found to be simple, accurate and incorporated in Anter FlashLine Equipment is Clark and Taylor correction factor (K_R). The Clark and Taylor correction factor includes the radiation heat losses, and is used in this research. Clark and Taylor examined the thermogram before system reached the maximum temperature. The correction factor is derived from taking time to reach 25% and 75% of the ΔT_{max} , where ΔT_{max} is maximum temperature rise on the back face. Then the correction factor K_R is given by:

$$K_R = -0.3461467 + 0.361578(t_{0.75}/t_{0.25}) - 0.06520543(t_{0.75}/t_{0.25})^2 \quad (2.3)$$

where K_R is the correction factor. The material diffusivity is given by:

$$\alpha_{corrected} = \frac{L^2}{t_{1/2}} K_R \quad (2.4)$$

The Clark and Taylor's correction factor was used in this research.

2.3.2 Flashline apparatus The essential components of the flashline apparatus are the laser flash source, specimen holder, temperature response detector, and recording device. These components are shown in Fig.2.2 in the block diagram along with data acquisition and analysis software. In addition, an environment control system is required to testing when the temperature is above and below the room temperature (ASTM E-1461, 2007). The flash source is generally a lamp or laser that can be able to beam quick energy pulse. The apparatus used in the research was Flashline™ 2000 by Anter Corporation. It has a high intensity xenon lamp as the pulse source. The pulse duration time should be less than 2% halftime of the specimen to be measured in order to keep the error due to finite pulse less than 0.5%. This equipment is able to test four specimens in one run. The samples are placed on sample change instrument in apparatus. Specimens are surrounded by furnace that increases the temperature of specimen. The technical specifications of equipment are listed in table 2.1.

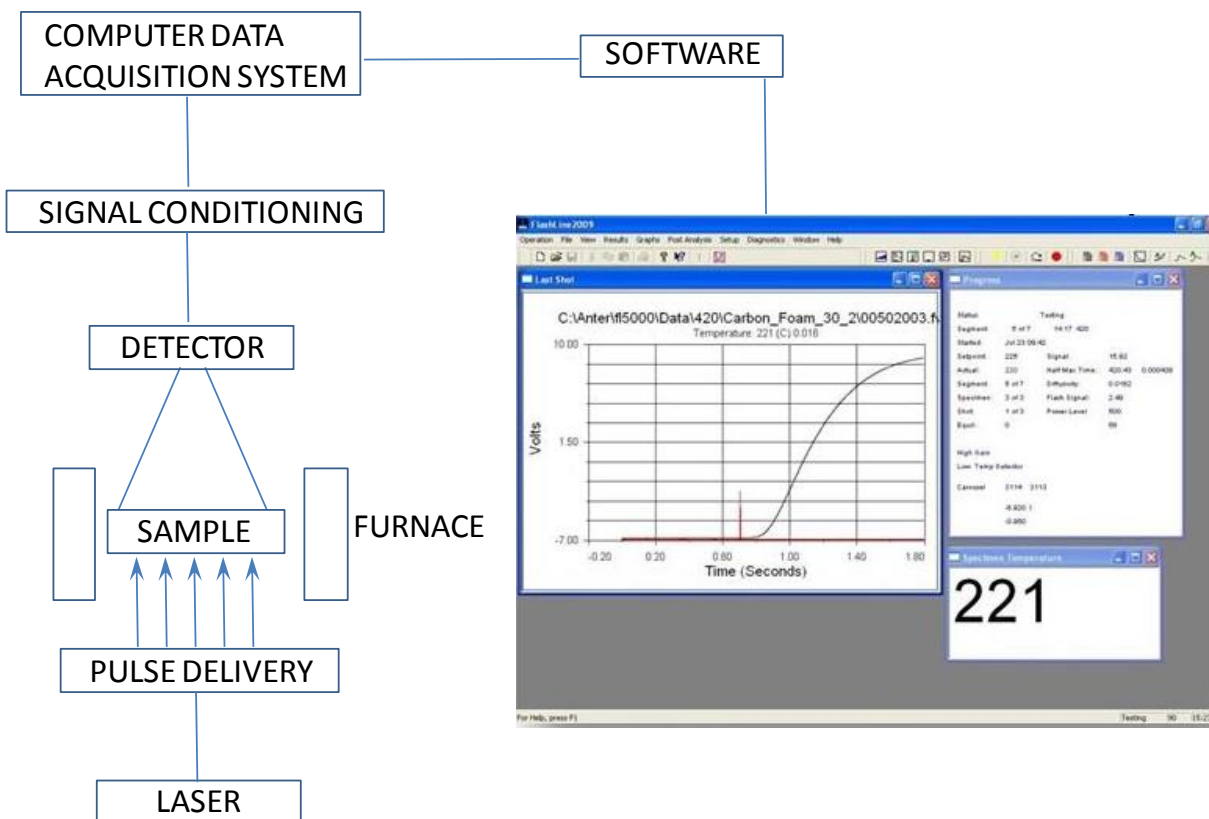


Figure 2.2 Block Diagram of a Flash System

Table 2.1

Technical Specifications of the FlashLine™ 2000 Thermal Properties Analyzer

<i>Flashline™ 2000 by Anter Corporation</i>	
<i>Pulse Source:</i>	High Speed Xenon Discharge
<i>Thermal Diffusivity Range:</i>	0.001 – 10 cm ² /s
<i>Operating Temperature Range:</i>	Room Temperature to 330°C
<i>Furnace:</i>	Nichrome Heaters
<i>Atmosphere:</i>	Air or Inert Gas Purge
<i>Interlock:</i>	Four Sample (Indexed) System
<i>Testing Samples:</i>	Cylindrical shape, 1 – 6 mm thick, 6 – 30 mm Diameter, wide range of materials and compositions
<i>Cooling System:</i>	LN ₂

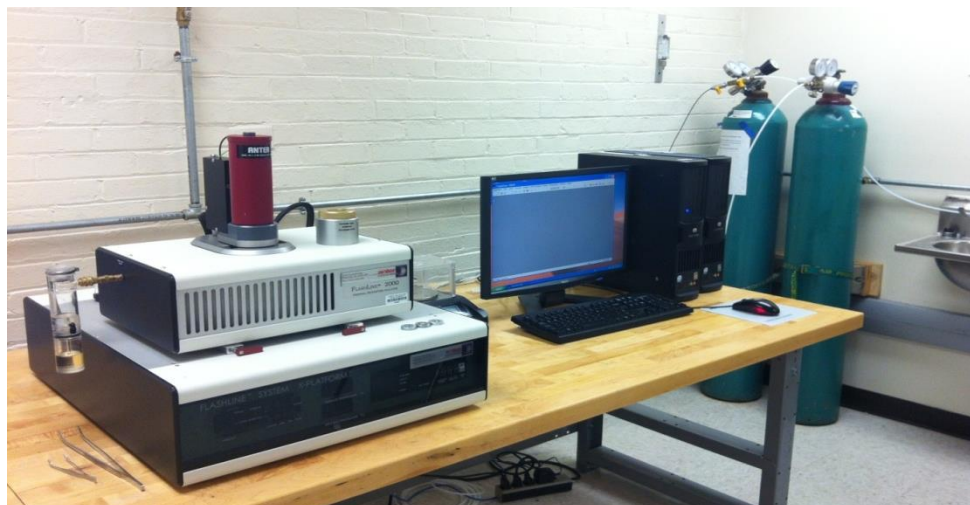


Figure 2.3 Experimental Setup for the Thermal Diffusivity measurement

The thermal property analyzer also has vacuum-capable environmental enclosure. Nitrogen gas is used as inert gas to evacuate chamber. The detector needs to identify any linear electrical output to a small temperature rise. The amplifier response time should be less than 2% of the half time. Indium Antimonide (InSb) detectors are very sensitive infrared detectors for thermal imaging systems. The InSb infrared detectors outputs a linear signal proportional to a small temperature change on the back face of the sample after the pulse applied on the front face.

2.3.3 Experimental procedure. ASTM E-1461 (2007) test standard was followed while conducting the experiments. Five of 12.5 mm diameter samples were prepared to make measurement of axial direction thermal diffusivity. Four of 12.5 mm diameter samples were prepared to measure the thickness direction thermal diffusivity. The diameter, thickness, mass, and density were measured and documented. Each sample was placed in the specimen holders inside a vacuum sealed environmental enclosure. Nitrogen gas was purged into the environmental enclosure as inert gas.

A large Dewar approximately 20L is filled with liquid nitrogen from Airgas, Inc. The liquid nitrogen in this large Dewar was poured into the small Dewar which is about 1 L. The

liquid nitrogen was manually poured in the receptacle of the IR detector. While running the experiment, IR detector was feed regularly with the liquid nitrogen. The measured specimen thickness, diameter, and mass were input into the FlashlineTM 2000 System, and test temperature program is set to the required value. The test was started from the room temperature and each sample was tested at different intervals to a maximum temperature of 100°C. At each temperature segment two to three flashes were performed at a time. The results were compiled, and analyzed, and corrections were made if necessary.

2.3.4 Calculation and correction. The Parker Equation (Equation 2.2) was used to calculate thermal diffusivity (α_p) by using the specimen thickness, L , and half-rise time $t_{1/2}$. Then, Clark and Taylor correction factor is applied to minimize heat loss deviation using the thermogram data. Thermogram data gives the plot of temperature rise versus time as shown in figure 2.4. Mathematical model is provided by ASTM E-1461 (2007). The figure 2.3 shows the difference between the mathematical model and experimental data.

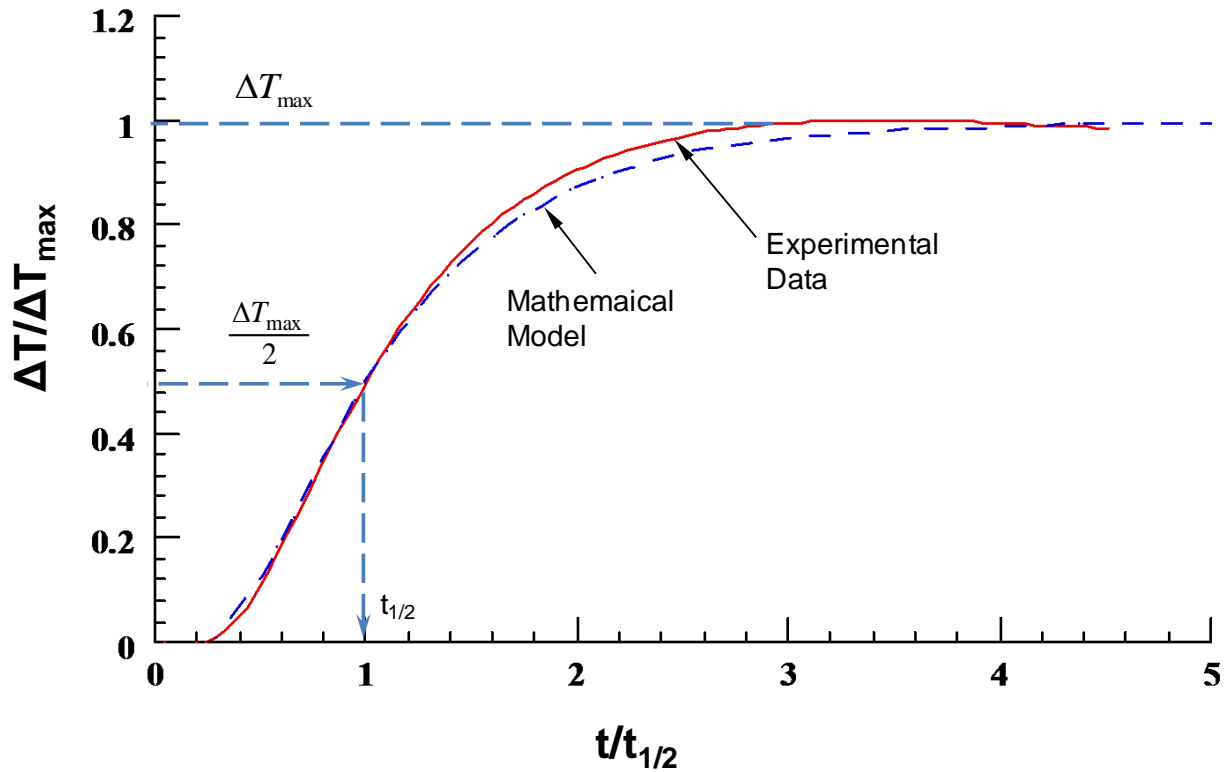


Figure 2.4 The Flash Method Thermogram

ΔT = Rise temperature in Celcius

$$\Delta T_{\max} = T_{\infty} - T_0$$

T_{∞} = Max temperature that diffusivity can get closed

T_0 = Initial Temperature

$t_{1/2}$ = time, s, required for the back face temperature to be one- half ΔT_{\max}

Experimental data and mathematical model give 3% variations for the Clark and Taylor correction factor.

2.4 Measurement of Specific Heat Capacity

Specific heat is the amount of heat required to raise the temperature of one gram of a material by one degree Celsius. Differential Scanning Calorimetry (DSC) is the most popular method to measurement of specific heat. The technique of DSC is based on comparing the heat

flow of the sample with the heat flow of a reference material whose properties are known in a controlled increasing temperature program (Höhne et al., 2003). DSC can determine how the specific heat of the sample varies with respect to the temperature using the data of the heat flow of the sample.

2.4.1 Differential Scanning Calorimetry model. Differential Scanning Calorimetry (DSC) is a thermo-analytical technique that is commonly used for specific heat measurement. DSC, in addition, can provide various properties of materials such as glass transition, melting points, crystallization time and temperature, rate and degree of cure, and oxidative/thermal stability (Blumm & Kaisersberger, 2001). Heat flow rate $\frac{dQ}{dt}$ and heating rate $\frac{dT}{dt}$ is measured using DSC, and then the measured data is used to calculate specific heat capacity of the unknown material using the equation 2.5 at constant pressure:

$$C_p = \frac{1}{m} \frac{dQ}{dT} \quad (2.5)$$

Where m is the mass of the material and $\frac{dQ}{dT}$ is the gradient of the heat flow with respect to the temperature T . Applying the chain rule of differentiation, specific heat can be written as:

$$C_p = \frac{1}{m} \frac{dt}{dT} \frac{dQ}{dt} \quad (2.6)$$

Machine constant (E_m) has a significant role in this measurement, since the precise measurement of $\frac{dQ}{dt}$ and $\frac{dT}{dt}$ are very difficult to measure and depends on equipment to equipment. The machine constant is determined using a C_p of a known material. The sapphire is used as reference material and E_m was determined to be 0.28 for the NETZSCH DSC 200 F3 Maia®. Then the C_p of a unknown material is calculated by:

$$C_p = \frac{\left(\frac{dQ}{dt}\right)}{m \left(\frac{dT}{dt}\right)} E_m \quad (2.7)$$

The E_m was calculated from separate test with the same equipment and a sapphire as a reference material, for which C_p is known. The following gives the value E_m :

$$E_m = \frac{m \left(\frac{dT}{dt}\right)}{\left(\frac{dQ}{dt}\right)} C_p \quad (2.8)$$

The experiment was conducted by setting the machine to operate from 20°C to 100°C with a set heating rate 0.25°C/s. The measured E_m was 0.28, and it was constant for a temperature range of 20°C to 100°C. This value is used to measure the C_p of the material of study.

2.4.2 DSC apparatus. The calorimeter used in this research is NETZCH DSC 200 F3 Maia®. The essential components of the apparatus consists of furnace, temperature sensor, differential sensor, and a test chamber environmental enclosure and temperature controller, recording device, containers, and cooler. This calorimeter uses the technique in which the difference in the heat flow to a sample and to a reference is observed as a function of time or temperature. It is a heat flux system that combines high stability, high resolution, fast response, and easiness to operate (NETZSCH, 2008). The NETZSCH DSC operates according to the ASTM E-1269 (2005).



Figure 2.5 DSC 200 F3 Maia®

The operation range is between -170°C to 600°C since it contains external cooler which improves the temperature range and allows the equipment to cool fast from raised temperatures to preferred temperatures. The furnace block surrounds sensor plate to arrange no temperature gradient difference occurs between reference and sample. The furnace, also, provides uniform and controlled heating. The heating range is between 0.001 K/min to 100 K/min . The figure 2.6 shows cross-sectional view of DSC 200 F3 Maia®.

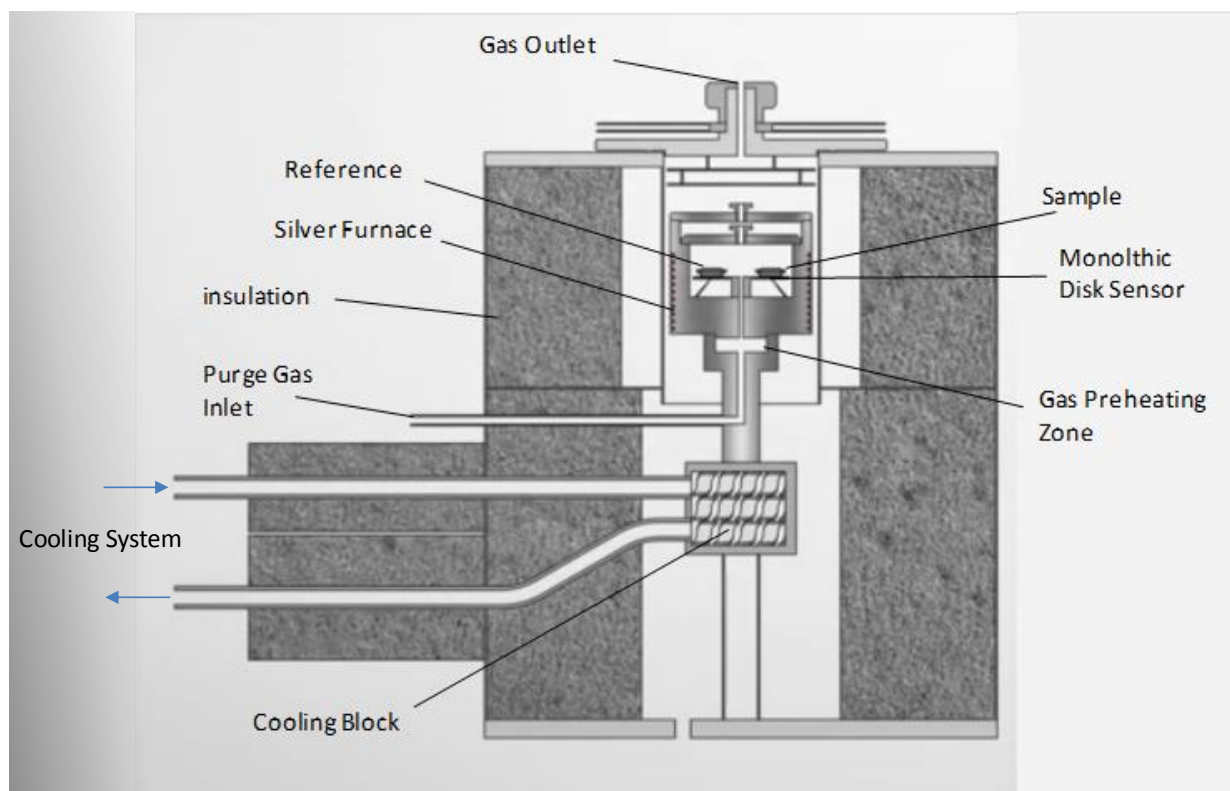


Figure 2.6 Cross-sectional view of DSC 200 F3 Maia®

The sample is placed in the pan and sealed with instrument's lid, and the three additional lids at the top to prevent influence of outside environment. External cooling system is used as temperature controller. The calorimeter contains high sensitive E type heat flux sensor for its experiments (NETZSCH, 2008).

2.4.3 Experimental procedure. Experimental procedure of DSC is according to the ASTM E-1269 (2005). The DSC 200 F3 Maia® Measuring Cell was opened. Proteus® Software was used to analyze the recorded data. The argon gas was used as inert gas and turned on to purge into the system. Gas purging rate was 40 ml/min which is enough to keep system in inert environment. Calibration test was done before starting to the test. The Indium (In) material with known mass was used for calibration of equipment. Three runs were performed in order to measure the specific heat of the unknown material.

Baseline and reference material were tested before the samples' tests. The aluminum crucibles are used inside of the apparatus to place the samples. Since the crucibles are contacting with samples, there is an additional contact resistance present. The baseline test corrects the contact resistance and increase the accuracy of the test. The baseline test must be applied same temperature program with the sample. The software was set to correction and temperature program was defined. Two empty crucibles were enclosed with lids and carefully carried into the reference and sample positions of the heat flux sensor. The crucibles were centered on the sensors. The figure 2.7 shows the crucibles on the heat flux sensor.

The program started at 20°C. Then, it cooled at a rate of 2°C/min to 5°C and was held there at least four minutes isothermally. The cell was heated to 120°C at a rate of 15°C/min and held isothermally for 5 minutes. The temperature program was cooled to 40°C and held there to get final ambient temperature. The equipment transmitted the heat signal to the data acquisition. The data acquisition gave thermal curves which show the thermal resistance versus temperature or time.

The calorimeter temperature was decreased to ambient temperature after the baseline run. The crucible on the sample location was taken out and sapphire reference material was placed into it. Then, the crucible was located on sample location again. The same program used for the baseline was executed for the sapphire reference. The mass of the reference material was inputted into the software before the test began. Following this test, the reference material was replaced with the specimen and the same procedure was repeated for the third time. The mass of the specimen was measured and input into the software. The data of heat flux of sapphire reference and specimen were recorded and saved in the software. The ratio method was used to

determine the specific heat of the material. This procedure was repeated for each sample material.

Table 2.2

Technical Specifications of NETZSCH DSC 200 F3 Maia

Technical Specifications of NETZSCH DSC 200 F3 Maia	
<i>Temperature Range:</i>	-170°C to 600°C
<i>Heating Rates:</i>	0.001°C/min to 100°C/min
<i>Cooling Rates:</i>	0.001°C/min to 100°C/min
<i>Sensor:</i>	E type heat flux System
<i>Measurement Range:</i>	0 mW to ± 600 mW
<i>Temperature Accuracy:</i>	0.1 K
<i>Enthalpy Accuracy:</i>	<1%
<i>Cooling Options:</i>	Intracooler
<i>Atmospheres:</i>	Inert gas (N ₂)

2.5 Validation of Methodology

Thermographite was tested to validate the results with literature (Maglić & Milošević, 2004).

Thermographite was selected because it is common reference material for flash method. The present test results varied between 0.1% and 5.3% literature data Plot of α vs T is shown in figure 2.7.

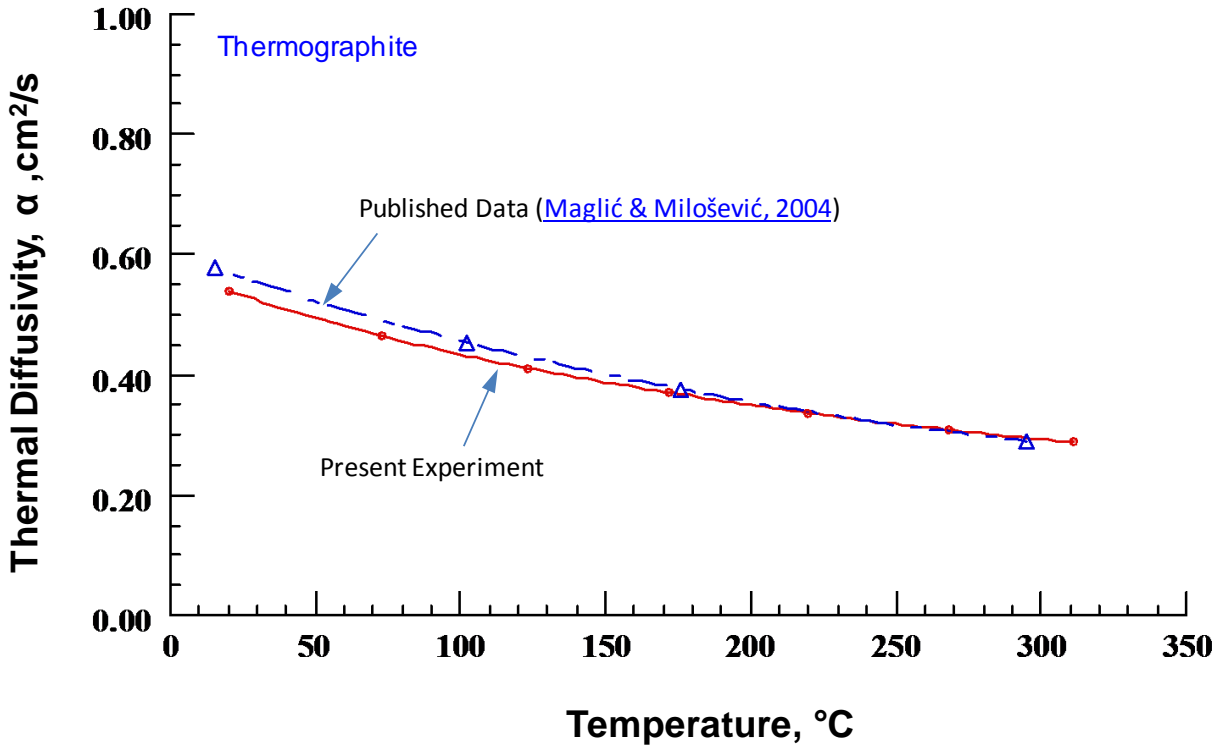


Figure 2.7 Validation of Flash Method with literature data

Sapphire (Al_2O_3) was chosen to validate the C_p method by DSC. The test was done and compared with the literature. The results shown in figure 2.8 the results vary between 2 % to 3.5% (Ditmars & Douglas, 1971).

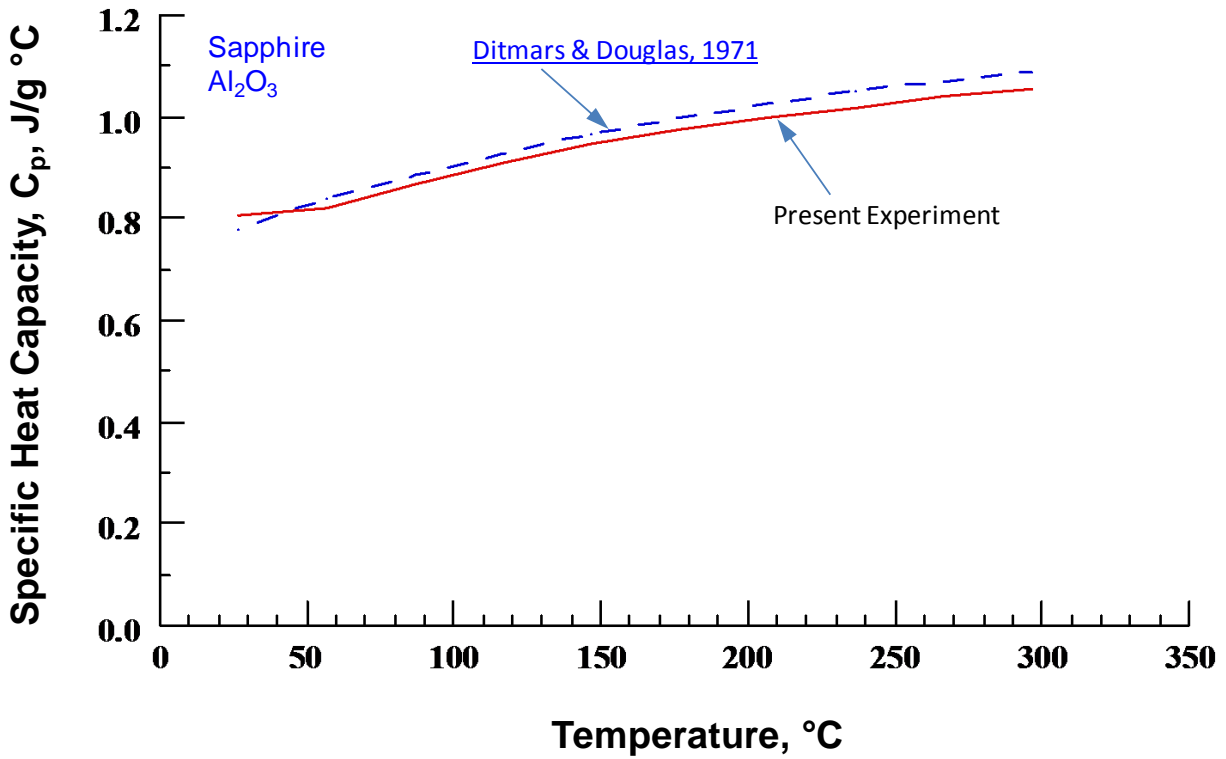


Figure 2.8 Validation of DSC with literature data

2.6 Preparation of Unidirectional Composite Test Samples

Thermal properties of fiber reinforced composites vary with in the directions of fiber. The axial and perpendicular directions of fiber formed the orthogonal principal directions for unidirectional composite materials. Therefore specimens are prepared in two different directions to measure axial and transverse conductivity. Thermal diffusivity changes with the direction of the fiber and can be measured by Anter FlashLine 2000 following ASTM E-1461 (2007). The density and specific heat capacity are scalar and they do not change with the direction. Therefore these properties are separately measured. The principal directions of fiber in the unidirectional composite material are shown in the figures 2.7 and 2.8. The axial and transverse directions are represented by x_1 , and x_2 (x_3) axes respectively. The thermal properties in x_2 and x_3 directions are

same, because of transverse isotropy of the plane x_2 - x_3 . Therefore specimen shown in figure 2.9 and 2.10 are used for measuring α_3 and α_1 , respectively, of the composite laminate.

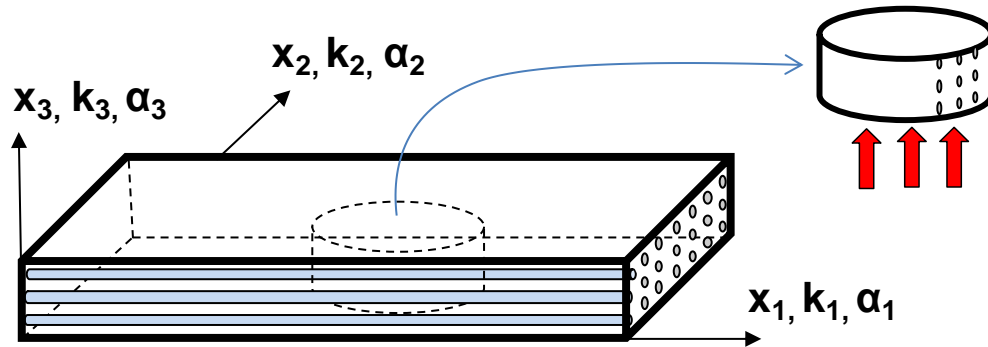


Figure 2.9 Transverse conductivity, and diffusivity ($k_2 = k_3$), ($\alpha_2 = \alpha_3$)

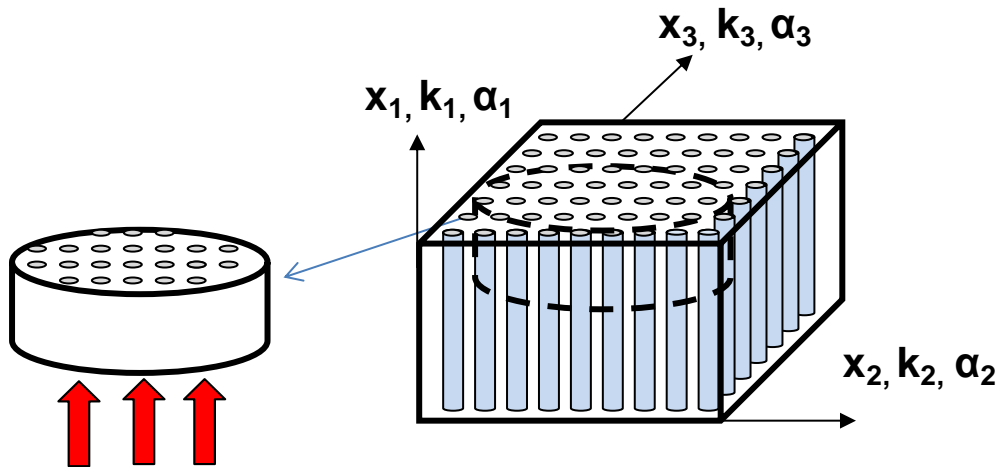


Figure 2.10 Axial conductivity, and diffusivity (k_1), (α_1)

2.7 Summary

An approach of determination of thermal conductivity of unidirectional fiber reinforced composite materials presented by measurement of thermal diffusivity, specific heat and material density. NETZSCH DSC 200 F3 Maia apparatus to measure the specific heat and Anter Flashline 2000 to measure thermal diffusivity were described. The description of the methodology and associated equations were summarized. In addition, preparing unidirectional

composite specimen to measure axial and transverse directions thermal conductivity was explained.

CHAPTER 3

IM7-G/8552 Carbon Epoxy Composite Materials

3.1 Introduction

In this chapter, fabrication of composite panel, directions of thermal property measurement and the associated specimen preparations are explained. Two types of specimens are prepared, axial and transverse where the fibers in parallel and perpendicular, respectively, to the direction of thermal conductivity determination.

3.2 Fabrication of Panels

Two IM7-G/8552 composite laminates were prepared for fabrication of test samples. One with 4-ply thick (0.648 mm) and 152.4 by 152.4 mm in-plane dimension and the other and 117-ply thick (19 mm) and is 76.2 by 76.2 mm size in-plane direction. The prepreg was supplied by Hexcel and laminate was fabricated using autoclave process as per the supplier specification at Center of Composite Material Research (CCMR), North Carolina Agricultural & Technical State University. The areal density of the carbon fibers used in prepreg was 160 g/m^2 and the density of carbon fiber is 1.78 g/cm^3 and the measured thickness of the thin panel is 0.64 mm and the thick panel is 19mm. The fiber volume fraction of the composite material was calculated using the equation:

$$V_f = \frac{A_f N}{10^3 \rho_f h} \quad (3.1)$$

Where V_f is the fiber volume fraction, N is the number of plies in the laminate, A_f is the fiber areal weight (g/m^2), and h is the laminate thickness (mm). Calculated V_f is 0.58 and 0.6 for transverse (thin) and axial (thick) direction, respectively, from the equation 3.1.

3.3 Principal Directions of Thermal Property Measurement

Two or more layers of unidirectional plies in same directions were stacked as a composite laminate to measure the thermal properties. The three principal directions of the lamina were x_1 , x_2 , and x_3 that represent the axial and two transverse direction of the fiber, as shown in figures 3.1 and 3.2. The thermal properties in x_2 - x_3 plane was same isotropic in all directions, therefore measuring x_1 and x_3 directions were enough to determine thermal conductivity of unidirectional composite material. Figure 3.1 and 3.2 also shows the thermal conductivity in principal directions. Since, the carbon fibers were more conductive than epoxy matrix, thermal conductivity the fiber direction (x_1) was more than through the transverse direction. The reason for this difference was because of difference in thermal diffusivity of fiber and matrix. Since the density and the specific heat capacity were scalar, they did not affect the thermal conductivity in terms of direction. However, the thermal diffusivity is the unique characteristic that thermal conductivity is related in fiber direction.

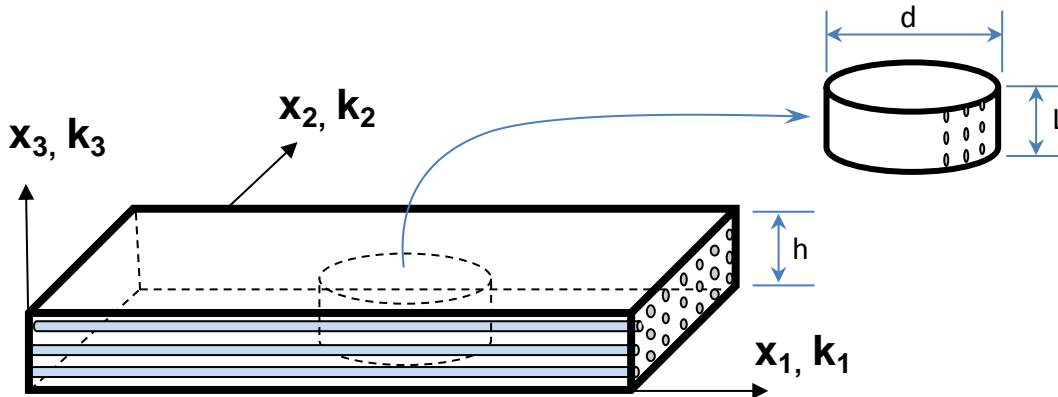


Figure 3.1 Through the thickness direction of IM7-G/8552 unidirectional composite material

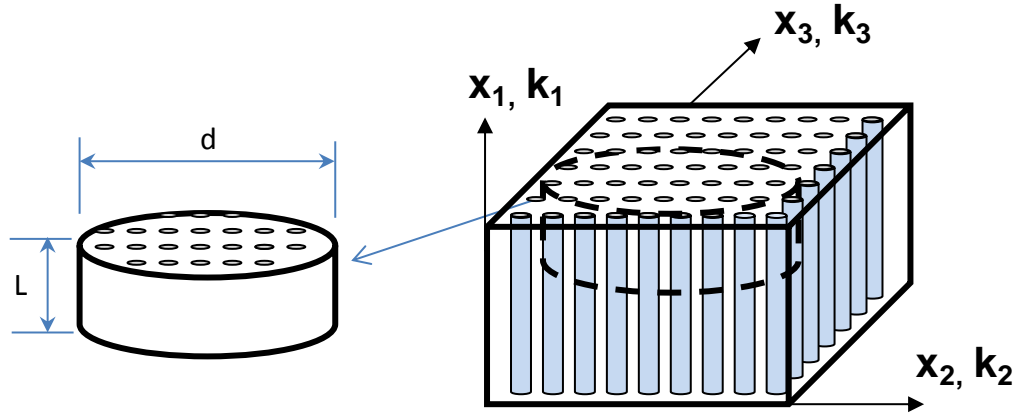


Figure 3.2 Axial direction of IM7-G/8552 unidirectional composite material

3.4 Specimen Preparation

The cylindrical samples of diameter 12.5 mm were cut in two different directions (x_1 and x_3) to measure thermal diffusivity along the x_1 and x_3 directions, respectively. Four samples were prepared for each case, the photograph of the specimens are in figure 3.3.a and 3.4.a, respectively, for transverse and axial diffusivity tests. Additionally, samples of 4 mm diameter and 1.5 mm thick were prepared for specific heat measurement.

3.4.1 Diffusivity measurement test samples. Four samples were cut and tested to determine the thermal diffusivity in through the thickness direction from the thin laminate (152.4 x 152.4 x 0.64 mm) five samples were cut for the axial direction thermal diffusivity from 76.2 x 76.2 x 19 mm thick laminate. The test specimens were prepared in thin 12.5 mm disk shapes. The area of the front faces must be smaller than that of the energy pulse beam (ASTM E-1461, 2007). The figure 3.3. through 3.6 show the model and photography of specimens prepared for through the thickness and axial direction.

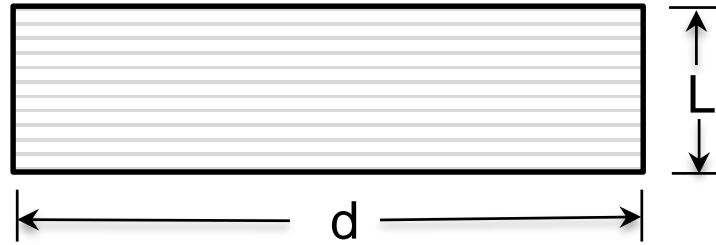


Figure 3.3 Specimen model of thermal diffusivity through the thickness (t-t) samples

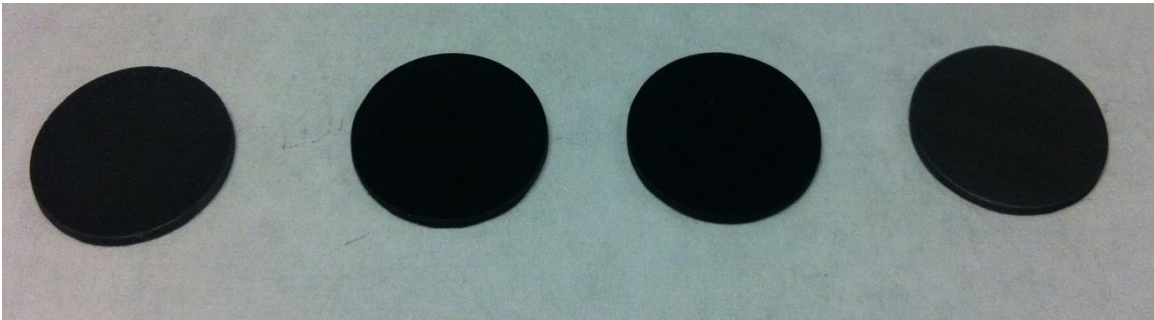


Figure 3.4 Photography of thermal diffusivity through the thickness (t-t) samples



Figure 3.5 Specimen model of thermal diffusivity axial direction samples

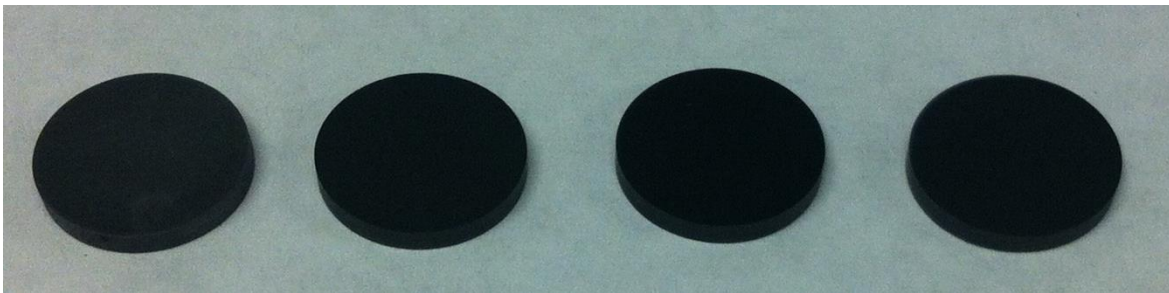


Figure 3.6 Thermal diffusivity axial direction samples

The optimum thickness (L) depends upon the magnitude of the estimated thermal diffusivity. The thickness should be chosen according to the half time, which should be between 10 to 1000 ms. In order to fulfill these dimensions, a milling machine drill press equipment was used to cut sample to proper thickness. Each of the specimens was hand sanded at the top and bottom faces to remove the mold release coat. All specimens were washed with ethanol, and then they were cleaned in an ultrasonic bath. Weight and the dimensions of the samples were measured, recorded and listed in the table 3.1. In this table, the specimen number is represented by S-T-# or S-A-#, where ‘S’ stand for specimen, ‘T’ for fiber transverse direction, and ‘A’ for fiber axial direction. The ‘#’ goes from 1 to 4 for transverse specimens and 1 to 5 for axial specimens.

Table 3.1

Physical properties of specimens

Test Specimen	Mass, mg	Diameter, mm	Thickness, mm	Density, mg/mm ³	V _f
S-T-1	122.76	12.60	0.62	1.59	0.58
S-T-2	123.85	12.54	0.63	1.59	0.58
S-T-3	124.01	12.61	0.62	1.59	0.58
S-T-4	117.91	12.54	0.60	1.58	0.56
S-A-1	388.23	12.56	1.98	1.58	0.60
S-A-2	389.81	12.57	1.99	1.58	0.60
S-A-3	389.67	12.56	1.99	1.58	0.60
S-A-4	388.37	12.56	1.98	1.58	0.60
S-A-5	388.72	12.56	1.99	1.58	0.60

3.4.2 Specific heat measurement test samples. The thermal contact between the heat flux sensor and the sample is significant for proper measurement of specific heat. The cylindrical specimens were machined to 4 mm diameter and 1.5 mm thickness. The top and bottom faces of

the specimen were precisely machined to maintain the flatness. The specimen's bottom face should be as flat as possible to achieve best contact with the crucible. The specimen mass, diameter and thickness were measured by microbalance and digital caliper and listed in table 3.2.

Table 3.2

Physical Specifications of Specimens

Test Specimen	Mass, mg	Diameter, mm	Thickness, mm
S-C _p -1	11.33	3.81	1.55
S-C _p -2	11.65	3.85	1.55
S-C _p -3	11.66	3.89	1.54
S-C _p -4	11.58	3.87	1.53
Sapphire (Al ₂ O ₃)	24.88	3.99	3.83

Sapphire (Al₂O₃) was used as a reference material to determine the machine constant, its geometry and found with the known mass are listed in table 3.2.

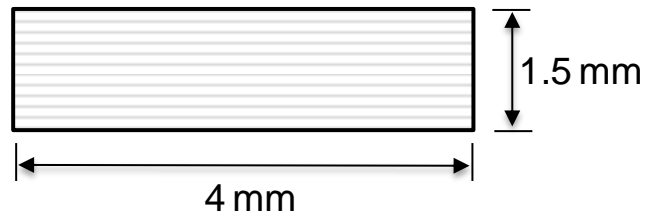


Figure 3.7 Specimen geometry of specific heat samples



Figure 3.8 Photograph of test samples

3.4.3 Optical microscopy of specimen. One of the specimen was tested for proper fiber orientation. This specimen was polished on the planes x_2 - x_3 and x_1 - x_3 planes to ensure direction of fiber for thermal diffusivity measurement. The optical images were taken to confirm the fiber directions. The specimen were polished using EcoMet® 250/300 supplied by BUEHLER. The lubricants, grades of abrasives, time, force, speed, and directions used are listed in table 3.3. After polishing, the specimen was cleaned and dried before taking the optical image.

Table 3.3

Polishing sequence, parameters and materials (Buehler Equipment Components)

Step	Surface	Lubricant	Abrasive	Time, min	Force	Speed, rpm	Direction
1	CARBIMET®	Water	SiC- 320 grit	Till Plane	5 lb	230	In Phase
2	CARBIMET®	Water	SiC- 600 grit	3:00	5 lb	230	In Phase
3	TEXMET®	NA	METADI SUPREME- 9 μ m	5:00	5 lb	130	Contra
4	TEXMET®	NA	METADI SUPREME- 3 μ m	5:00	5 lb	130	Contra
5	MICROCLOTH®	NA	MASTERPREP®- 0.05 μ m	3:30	5 lb	130	Contra

Nikon Eclipse LV150 Microscope (see Fig 3.9) was used for imaging the specimens.

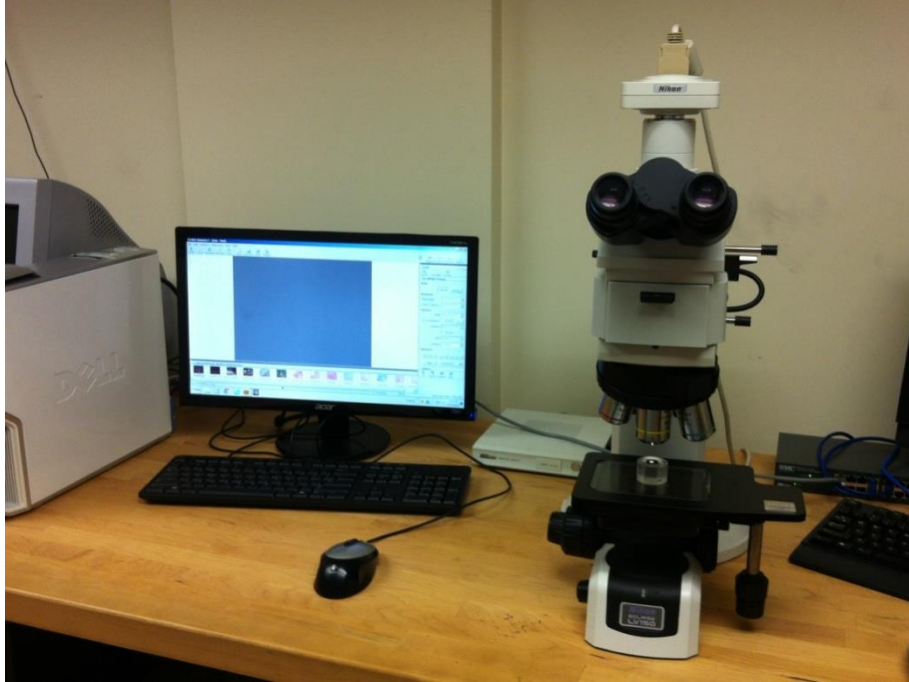


Figure 3.9 Nikon Eclipse LV150

The optical image of x_1 - x_2 and x_2 - x_3 planes of thin specimen (used for transverse diffusivity test) and thick (used for axial diffusivity test), are shown in Figure 3.10 and 3.11, respectively. Each image were magnified x20 and x50 , respectively. The figures show the fibers perpendicular and parallel to the direction of diffusivity measurement.

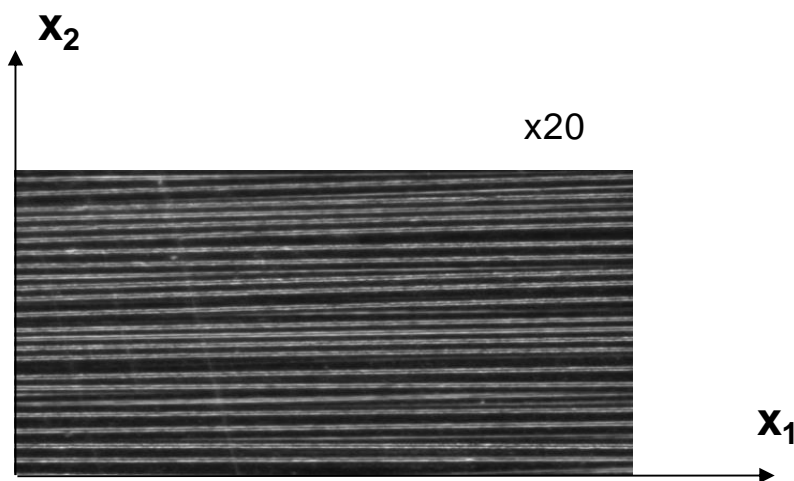


Figure 3.10 Optical image of x_1 - x_2 planes the thin specimen for transverse diffusivity measurement in x20 magnification

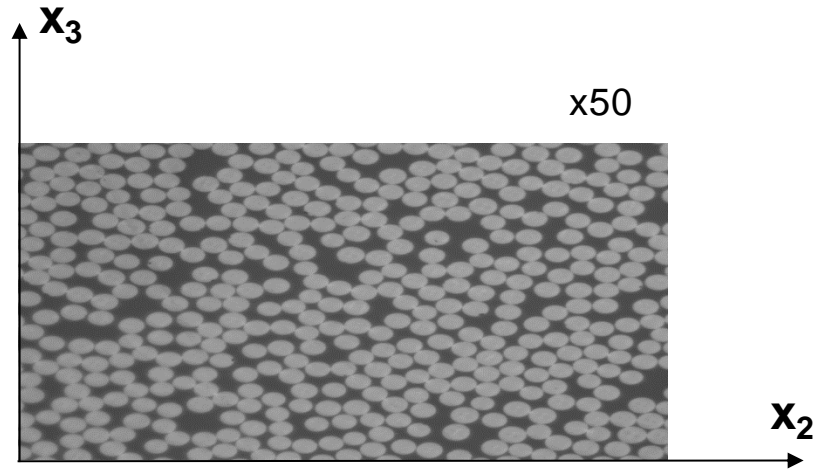


Figure 3.11 Optical images of x_2 - x_3 plane of the thick samples for axial diffusivity measurement in x50 magnification

3.4.4 Specimens for special study. Although the specific heat is a material property independent of specimen shape, this was reconfirmed for IM7-G/8552-2 carbon/epoxy composite. Three types of specimen, about the same mass, were selected: Square (Sq), rectangular (Re), and circular (Cr). The mass and geometry of all 12 specimen are listed in Table 3.4. Specific heat of these specimen were measured separately to confirm the independence of this property.

Table 3.4 Physical Properties of Special Assessment Specimens

Test Specimen	Mass, mg	Diameter, mm	Length, mm	Width, mm	Thickness, mm
S-Sq-1	33.60	-	3.94	3.95	1.40
S-Sq-2	33.61	-	3.93	3.93	1.42
S-Sq-3	33.64	-	3.95	3.92	1.43
S-Sq-4	33.00	-	3.94	3.92	1.39
S-Sq-5	33.43	-	3.94	3.92	1.40
S-Re-1	28.25	-	4.53	2.98	1.34
S-Re-2	27.80	-	4.53	2.99	1.31
S-Re-3	27.99	-	4.53	3.00	1.32
S-Re-4	28.15	-	4.54	3.00	1.33
S-Re-5	28.90	-	4.52	3.00	1.37
S-Cr-1	25.84	3.95	-	-	1.40
S-Cr-2	26.16	3.95	-	-	1.41

The figure 3.12 and 3.13 show the cutted sample for shape effect



Figure 3.12 Square Shape Samples



Figure 3.13 Rectangular Shape Samples

3.5 Summary

IM7-G/8552 unidirectional composite laminate was fabricated by autoclave process as per the prepreg supplier specification at the Center of Composite Material Research (CCMR), NCA&TSU. Two sets of specimens were prepared to measure two different directions of diffusivity and one set for specific heat. All geometric properties were measured to verify the proper orientation of fiber, a typical specimen was polished and optical images were taken and recorded.

CHAPTER 4

Experiment and Results

4.1 Introduction

This chapter presents an experimental measurement of thermal diffusivity of IM7-G/8552 carbon fiber composite along fiber and transverse to fiber directions, followed by the measurement of composite's specific heat. Using these properties thermal conductivities of the composite along and transverse directions are calculated. Thermal properties are measured over a temperature range of 20°C to 100°C to establish the conductivity and temperature relation. Room temperature properties of IM7-G/8552 are compared with the other carbon fiber/epoxy composites to assure the consistence and reasonableness of material properties.

4.2 The Measurement of Thermal Diffusivity

The thermal diffusivity tests were made using Anter Flashline 2000. Equipment thermal diffusivity tests transverse and axial directions of the fiber were measured, as explained previously, in two different directions of the fiber reinforced composites. Four samples were tested in transverse fiber direction and five samples were tested in axial direction of fiber. The diameter, thickness, mass, and density of all samples were measured and documented. The thickness was chosen according to the half time within the 10 to 1000 ms range (ASTM E-1461, 2007). The figure 4.1 shows the FlashLine™ 2000.

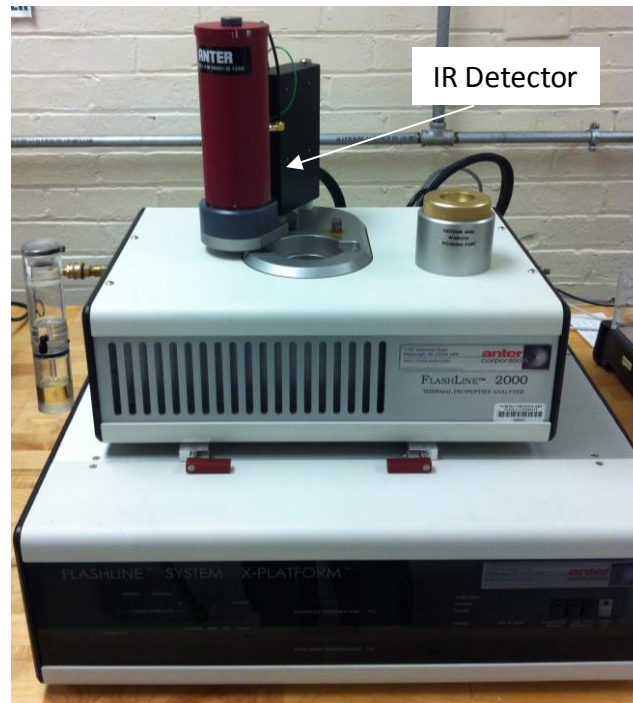


Figure 4.1 The FlashLine™ 2000

The nominal diameter of the test specimens were about 12.54 mm and the thickness about 0.62 and 1.98 mm for transverse and axial thermal diffusivity samples, respectively. First, the diffusivity was calculated according to Parker's Equation and Clark and Taylor's correction factor was applied to minimize the radiation effect. The software was started before the test and input data such as thickness, diameter, and density are entered. The equipment allows four specimens to be tested at one time. Each sample was placed in the specimen holders inside a vacuum sealed environmental enclosure. Nitrogen gas was purged into the environmental enclosure as inert gas. The gas flowed into the system at 0.034 N/mm^2 . The liquid nitrogen was manually poured in the receptacle of the IR detector to prevent from overheating. The samples were placed into the furnace by helping of tweezers. The thermal diffusivity of the composite material was measured between room temperature and 100°C , less than glass transition temperature of IM7-G/8552 composite material. This range was selected due to the temperature

limitations of the composite material. The specimens and the specimen holders are shown in Figure 4.2.



Figure 4.2 The FlashLine™ 2000 specimen holders and specimens

4.2.1 Axial thermal diffusivity. Axial orientation the fiber composite with respect to the test was important to get accurate measurement of thermal diffusivity and then conductivity of specimen. The axial samples shown in figure 3.6.b and were tested for axial diffusivity. The tests were performed from room temperature to 100°C. The measured diffusivity of samples are listed in tables 4.1 through 4.3. For all five samples half time ($t_{1/2}$), and the calculated Parker's diffusivity (α_{1p}), and Clark and Taylor corrected diffusivity (α_1) are listed in the tables for temperature range of 22°C to 98°C. The half time is within the ASTM limits (0 to 1 s) the essential parameter for diffusivity.

Table 4.1

The half time and axial thermal diffusivity values of sample 1 and sample 2

Temp, T °C	S-A-1, L= 1.98mm, $\rho=1.58\text{g/cm}^3$			S-A-2, L= 1.99mm, $\rho=1.58\text{g/cm}^3$		
	Half time $t_{1/2}$, s	Parker, α_{1P} , cm^2/s	Clark- Taylor, α_1 , cm^2/s	Half time $t_{1/2}$, s	Parker, α_{1P} , cm^2/s	Clark- Taylor, α_1 , cm^2/s
21	0.1559	0.0350	0.0344	0.1561	0.0351	0.0346
29	0.1561	0.0349	0.0351	0.1561	0.0351	0.0347
37	0.1561	0.0349	0.0346	0.1562	0.0351	0.0345
46	0.1575	0.0346	0.0340	0.1577	0.0347	0.0342
56	0.1587	0.0343	0.0339	0.1588	0.0345	0.0339
67	0.1591	0.0342	0.0336	0.1590	0.0344	0.0337
77	0.1597	0.0341	0.0333	0.1595	0.0343	0.0337
88	0.1607	0.0339	0.0333	0.1607	0.0341	0.0336
98	0.1618	0.0336	0.0330	0.1618	0.0339	0.0336

Table 4.2

The half time and axial thermal diffusivity values of sample 3 and sample 4

Temp, T °C	S-A-3, L= 1.99mm, $\rho=1.58\text{g/cm}^3$			S-A-4, L=1.98mm, $\rho=1.58\text{g/cm}^3$		
	Half time $t_{1/2}$, s	Parker, α_{1P} , cm^2/s	Clark- Taylor, α_1 , cm^2/s	Half time $t_{1/2}$, s	Parker, α_{1P} , cm^2/s	Clark- Taylor, α_1 , cm^2/s
22	0.1571	0.0348	0.0342	0.1577	0.0346	0.0344
29	0.1552	0.0352	0.0346	0.1582	0.0345	0.0339
38	0.1556	0.0351	0.0344	0.1589	0.0344	0.0339
46	0.1559	0.0351	0.0345	0.1599	0.0342	0.0336
57	0.1570	0.0348	0.0342	0.1614	0.0339	0.0332
67	0.1575	0.0347	0.0340	0.1606	0.0340	0.0334
78	0.1594	0.0343	0.0343	0.1621	0.0337	0.0335
89	0.1635	0.0334	0.0341	0.1649	0.0331	0.0342
99	0.1616	0.0338	0.0352	0.1624	0.0336	0.0330

The table 4.4 summarizes the axial diffusivity (α_l) for all samples, average values, standard deviation, and percent coefficient of variation are listed in the last three columns.

Table 4.3

The half time and axial thermal diffusivity values of sample 5

Temp, T °C	S-A-5, L= 1.99mm, $\rho=1.58\text{g/cm}^3$		
	Half time $t_{1/2}$, s	Parker, α_{1P} , cm^2/s	Clark- Taylor, α_1 , cm^2/s
22	0.1544	0.0355	0.0345
29	0.1552	0.0353	0.0346
38	0.1572	0.0348	0.0346
46	0.1575	0.0347	0.0342
57	0.1584	0.0346	0.0339
67	0.1582	0.0346	0.0342
78	0.1623	0.0337	0.0344
89	0.1644	0.0333	0.0324
99	0.1599	0.0342	0.0338

Table 4.4

Summary axial thermal diffusivity and average values of IM7-G/8552

Temp, T °C	Diffusivity, α_1 , cm^2/s						STD	% CV
	S-A-1	S-A-2	S-A-3	S-A-4	S-A-5	Average		
22	0.0344	0.0346	0.0342	0.0344	0.0345	0.0344	0.0001	0.4
29	0.0351	0.0347	0.0346	0.0339	0.0346	0.0346	0.0004	1.3
38	0.0346	0.0345	0.0344	0.0339	0.0346	0.0344	0.0003	0.8
46	0.0340	0.0342	0.0345	0.0336	0.0342	0.0341	0.0003	1.0
57	0.0339	0.0339	0.0342	0.0332	0.0339	0.0338	0.0004	1.1
68	0.0336	0.0337	0.0340	0.0334	0.0342	0.0338	0.0003	0.9
78	0.0333	0.0337	0.0343	0.0335	0.0344	0.0338	0.0005	1.4
89	0.0333	0.0336	0.0341	0.0342	0.0324	0.0335	0.0007	2.2
99	0.0330	0.0336	0.0352	0.0330	0.0338	0.0337	0.0009	2.7

Figure 4.3 shows the plot of thermal diffusivity versus temperature of IM7-G/8552 composite. Average value and the specimen data are shown in the plot. The thermal diffusivity nearly constant over the temperature range but it shows a small decrease with the temperature. The least square linear regression analysis fit is given by:

$$\alpha_1 = 0.035 - 10^{-5}T \quad (4.1)$$

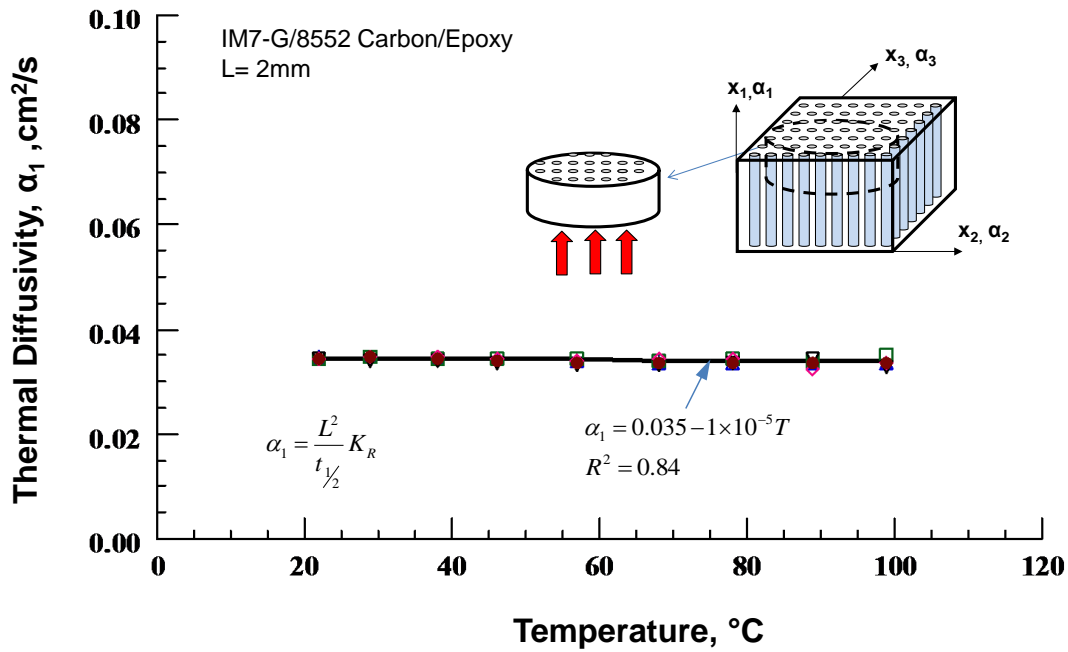


Figure 4.3 Axial thermal diffusivity diagram of IM7-G/8552(5 Samples)

The statistical analysis was used to define the error based on normal distribution and 95% confidence. Statistical analysis was performed based on Figliola and Beasley (2011) and the results are summarized. The population standard deviation (STD) is given by:

$$STD = \sqrt{\frac{1}{N} \sum_{i=1}^N (a_i - \bar{a})^2} \quad (4.2)$$

In that equation, N is the total number of measurements, a_i represents a single i^{th} measurement, and \bar{a} is the mean value of the data at each temperature. Standard error (SE) was calculated for each temperature using standard deviation of the mean:

$$SE = \frac{STD}{\sqrt{N}} \quad (4.3)$$

The critical value from the normal distribution chart based on 95% confidence is 1.96, and the margin of error, e , is determined by the following equation:

$$e = \pm 1.96 \times SE \quad (4.4)$$

The percent error is defined by:

$$\text{Percent error} = \frac{e}{\text{mean}} \times 100\% \quad (4.5)$$

The results for the conductivity and the percent error for the corresponding temperature values were calculated and are listed in Table 4.5. The plot of the error and standard deviation are given in Figure 4.4.

Table 4.5

Percent error of thermal diffusivity in axial direction

Temp, T °C	Average, cm²/s	STD	e	<i>Percent error</i>
22	0.0344	0.0001	0.0001	0.4
29	0.0346	0.0004	0.0004	1.1
38	0.0344	0.0003	0.0003	0.7
46	0.0341	0.0003	0.0003	0.9
57	0.0338	0.0004	0.0003	1.0
68	0.0338	0.0003	0.0003	0.8
78	0.0338	0.0005	0.0004	1.3
89	0.0335	0.0007	0.0006	1.9
99	0.0337	0.0009	0.0008	2.3

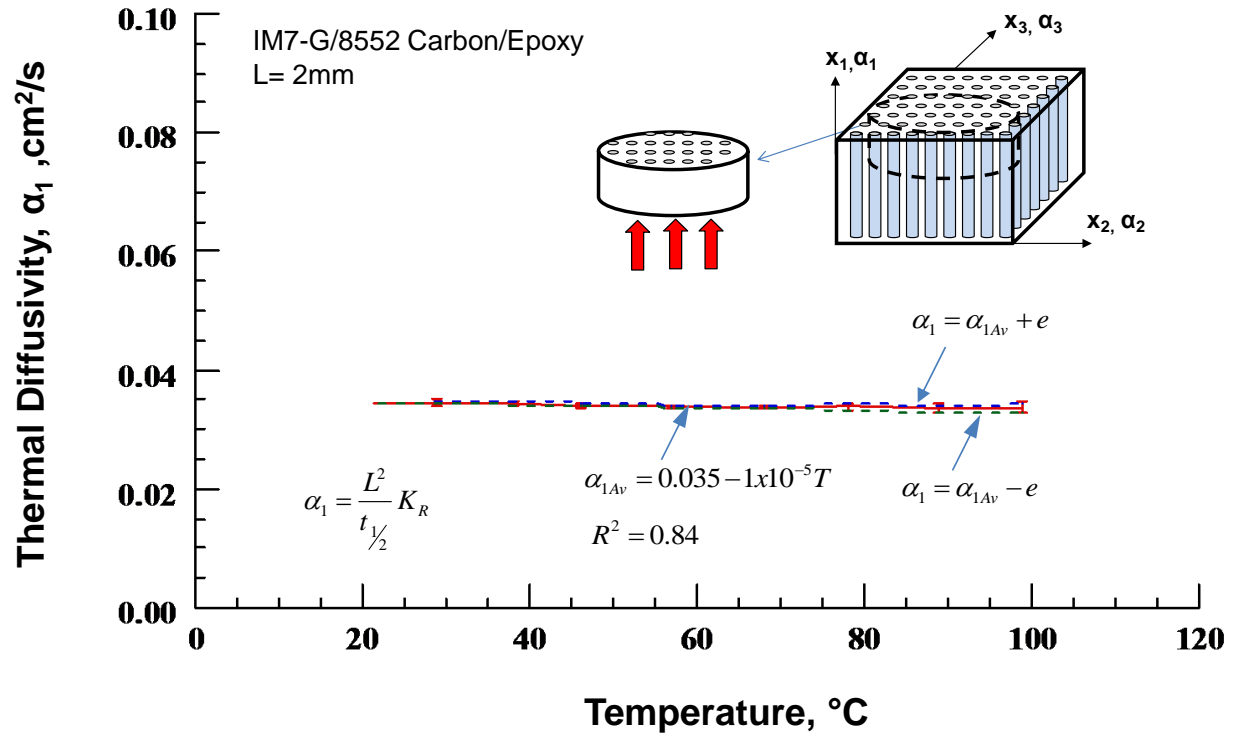


Figure 4.4 Error diagram of axial thermal diffusivity test

4.2.2 Transverse thermal diffusivity (α_3). Transverse diffusivity was measured with Anter Flashline 2000. Laser flash was subjected in perpendicular to the fiber direction. x_2 and x_3 directions were same because they both are perpendicular to the fibers. x_3 direction was chosen and test was run to measure transverse thermal diffusivity. The thermal diffusivity and half-time values of the experiment in axial direction were given previously. Transverse thermal diffusivity values were lower than the axial thermal diffusivity since carbon fibers are more conductive than the matrix and fibers extended constantly from one side to other side in axial direction of unidirectional composite materials. Half-time to reach to the maximum temperature is an important parameter and should be in the 10 to 1000ms range according to the ASTM E-1461 (2007). Half-time, thickness, Parker equation, and Clark-Taylor correction factor measurements are given in the Table 4.6 and 4.7.

Table 4.6

Transverse thermal diffusivity data of sample 1 and sample 2 of IM7-G/8552

Temp, T °C	S-T-1, L= 0.63mm, $\rho=1.56\text{g/cm}^3$			S-T-2, L=0.63mm, $\rho=1.58\text{g/cm}^3$		
	Half time $t_{1/2}$, s	Parker, α_{3P} , cm^2/s	Clark- Taylor, α_3 , cm^2/s	Half time $t_{1/2}$, s	Parker, α_{3P} , cm^2/s	Clark- Taylor, α_3 , cm^2/s
22	0.1280	0.0043	0.0041	0.1377	0.0041	0.0038
29	0.1292	0.0043	0.0041	0.1390	0.0040	0.0038
38	0.1307	0.0042	0.0040	0.1405	0.0040	0.0038
46	0.1318	0.0042	0.0040	0.1416	0.0039	0.0037
57	0.1333	0.0041	0.0039	0.1435	0.0039	0.0037
68	0.1349	0.0041	0.0039	0.1450	0.0038	0.0036
78	0.1360	0.0040	0.0038	0.1465	0.0038	0.0036
89	0.1374	0.0040	0.0038	0.1481	0.0038	0.0036
99	0.1375	0.0040	0.0038	0.1480	0.0038	0.0036

Table 4.7

Transverse thermal diffusivity data of sample 3 and sample 4 of IM7-G/8552

Temp, T °C	S-T-3, L= 0.64mm, $\rho=1.55\text{g/cm}^3$			S-T-4, L= 0.61mm, $\rho=1.57\text{g/cm}^3$		
	Half time $t_{1/2}$, s	Parker, α_{3P} , cm^2/s	Clark- Taylor, α_3 , cm^2/s	Half time $t_{1/2}$, s	Parker, α_{3P} , cm^2/s	Clark- Taylor, α_3 , cm^2/s
21	0.1333	0.0043	0.0041	0.1122	0.0045	0.0044
29	0.1481	0.0039	0.0039	0.1132	0.0045	0.0043
38	0.1418	0.0040	0.0038	0.1145	0.0044	0.0043
46	0.1434	0.0040	0.0038	0.1159	0.0044	0.0042
57	0.1473	0.0039	0.0038	0.1166	0.0043	0.0042
67	0.1471	0.0039	0.0038	0.1184	0.0043	0.0042
78	0.1505	0.0038	0.0038	0.1184	0.0043	0.0041
89	0.1508	0.0038	0.0037	0.1202	0.0042	0.0041
99	0.1509	0.0038	0.0036	0.1212	0.0042	0.0041

The experiment was conducted between room temperature and 100°C. Axial thermal diffusivity was approximately 8.5 times more than transverse thermal diffusivity. The diffusivity in transverse direction decreases with increasing the temperature. Transverse thermal diffusivity (α_3) decreases against to temperature. Average value of the 4 specimens is close to the linear curve. Figure 4.5 illustrates the data of all specimens and the average value of those specimens at each temperature. Equation of the average value of α_3 is determined by least square linear regression, and the equation is:

$$\alpha_3 = 0.0042 - 4 \times 10^{-5} T \quad (4.6)$$

Table 4.8

Transverse thermal diffusivity and average data of IM7-G/8552

Temp, T °C	Diffusivity, α_3 , cm ² /s					STD	% CV
	S-T-1	S-T-2	S-T-3	S-T-4	Average		
22	0.0041	0.0038	0.0041	0.0044	0.0041	0.0002	6.0
29	0.0041	0.0038	0.0038	0.0043	0.0040	0.0002	6.1
38	0.0040	0.0038	0.0038	0.0043	0.0040	0.0002	5.9
46	0.0040	0.0037	0.0038	0.0042	0.0039	0.0002	5.6
57	0.0039	0.0037	0.0038	0.0042	0.0039	0.0002	5.5
68	0.0039	0.0036	0.0038	0.0042	0.0039	0.0003	6.5
78	0.0038	0.0036	0.0037	0.0041	0.0038	0.0002	5.7
89	0.0038	0.0036	0.0036	0.0041	0.0038	0.0002	6.3
99	0.0037	0.0035	0.0036	0.0041	0.0037	0.0003	7.1

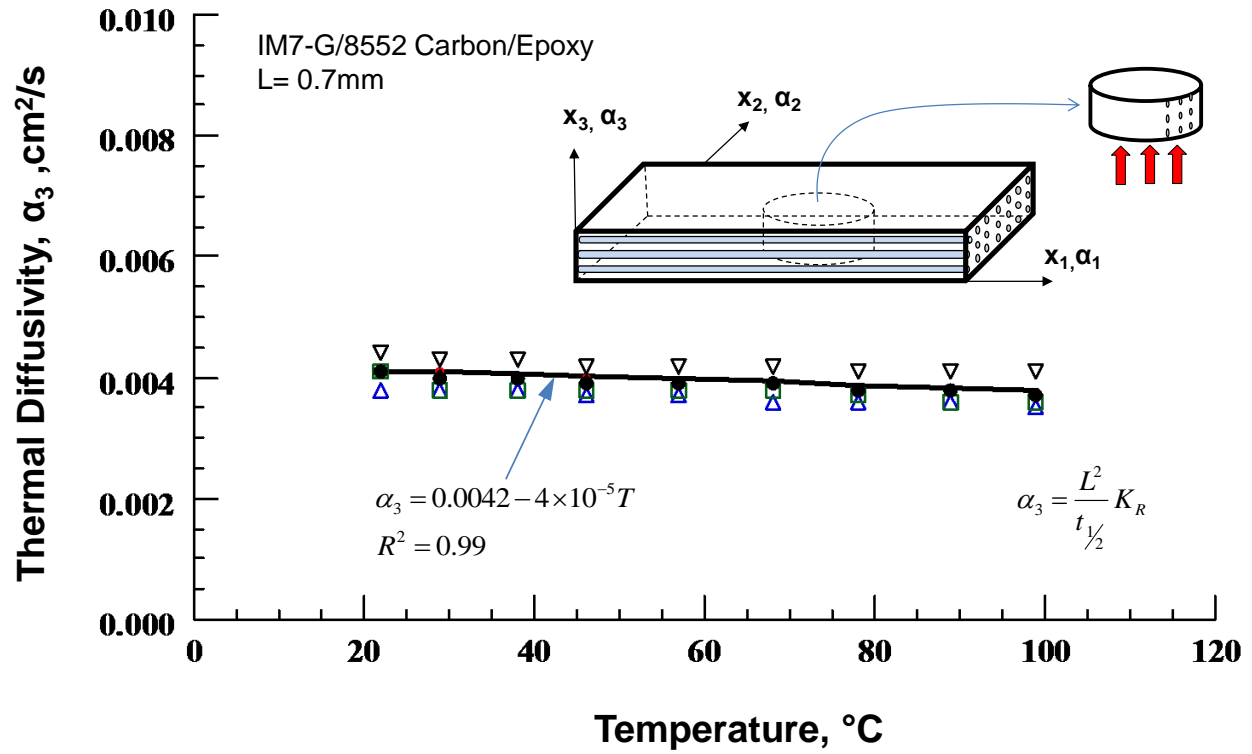


Figure 4.5 Transverse thermal diffusivity of IM7-G/8552(4 Samples)

The statistical analysis of the test is made and the results are presented in table 4.9 and figure 4.6.

Table 4.9

Percent error of thermal diffusivity in transverse direction

Temp, T °C	Average, cm ² /s	STD	<i>e</i>	Percent error
22	0.0041	0.0002	0.0002	5.2
29	0.0040	0.0002	0.0002	5.4
38	0.0040	0.0002	0.0002	5.2
46	0.0039	0.0002	0.0002	5.0
57	0.0039	0.0002	0.0002	4.9
68	0.0039	0.0003	0.0002	5.7
78	0.0038	0.0002	0.0002	5.0
89	0.0038	0.0002	0.0002	5.5
99	0.0037	0.0003	0.0002	6.2

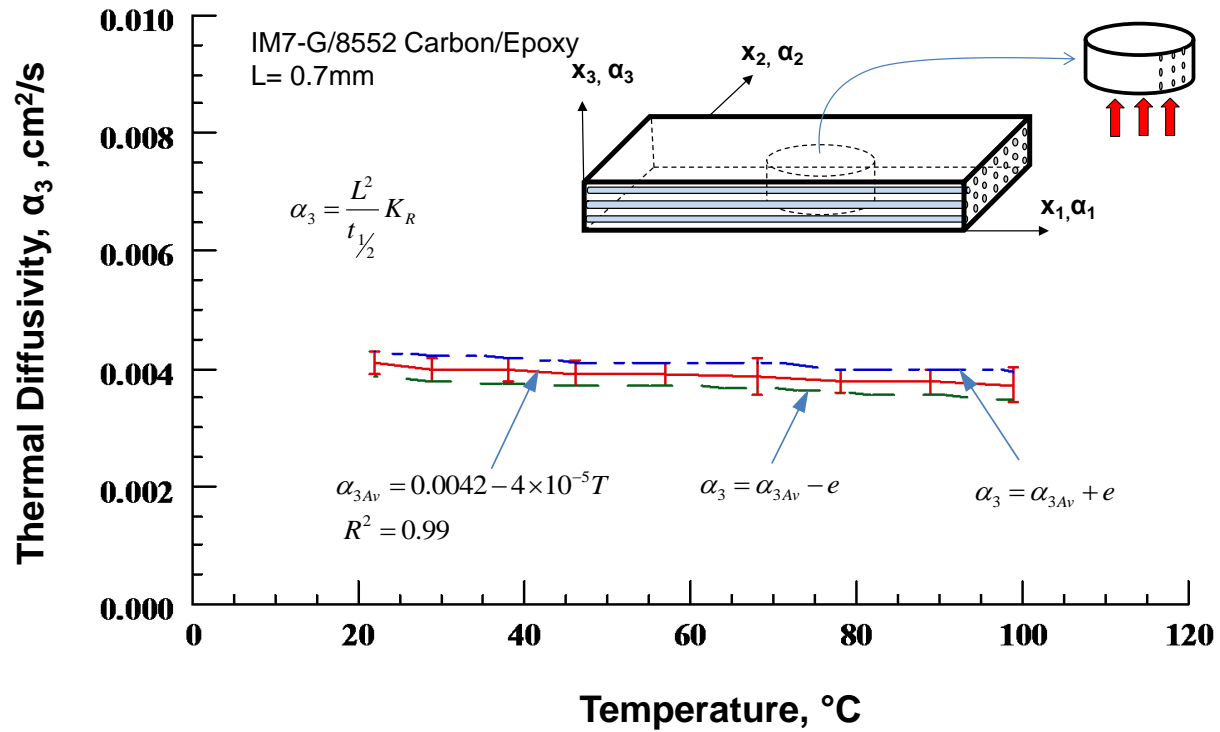


Figure 4.6 Error Bars of transverse thermal diffusivity measurement

4.3 Measurement of Specific Heat (C_p)

The specimens were prepared using 4-ply thick (0.648 mm) and 152.4 by 152.4 mm in-plane dimension IM7-G/8552 unidirectional composite laminate to measure specific heat capacity. Four specimens were prepared in 4 mm diameter and 0.624 mm thickness to fit inside of the crucibles. Measurement of specific heat methodology is given by ASTM E1269 (2005). The test was conducted from room temperature (22°C) to 100°C at heating rate of 15°C/min and collected data interval about 10°C. The data acquisition system was calculated the C_p at each temperature and that was calculated by Equation 2.7. To make measurement with DSC, a test specimen and reference were located on a metallic block with high thermal conductivity and closed to the same furnace in the calorimeter. The importance of metal block is to ensure the heat

flow path between the specimen and reference. The reference is an inert material such as alumina, or just an empty pan. The temperature of sample and the reference were increased at identical constant rate. The changes in the specific heat led to a difference of temperature and heat flux relative to the reference. The DSC calculated the specific heat capacity of tested sample using the heat flow data by ratio method technique. The change in enthalpy of reference to the heat absorbed or released by reference because the DSC is at constant temperature (ASTM E-1269, 2005).

The test was four steps including calibration. The Indium (In) material was used to calibrate the equipment. As the first step, in material's melting point was determined by the equipment to calibrate. The equipment's results were exactly matched with the In data. Second step was the baseline test. Baseline test needed to be conducted to set the reference material and unknown material in same baseline. To achieve this, two empty pan were placed into on to the furnace block in the equipment. The picture of the pans and furnace block is in figure 4.7.

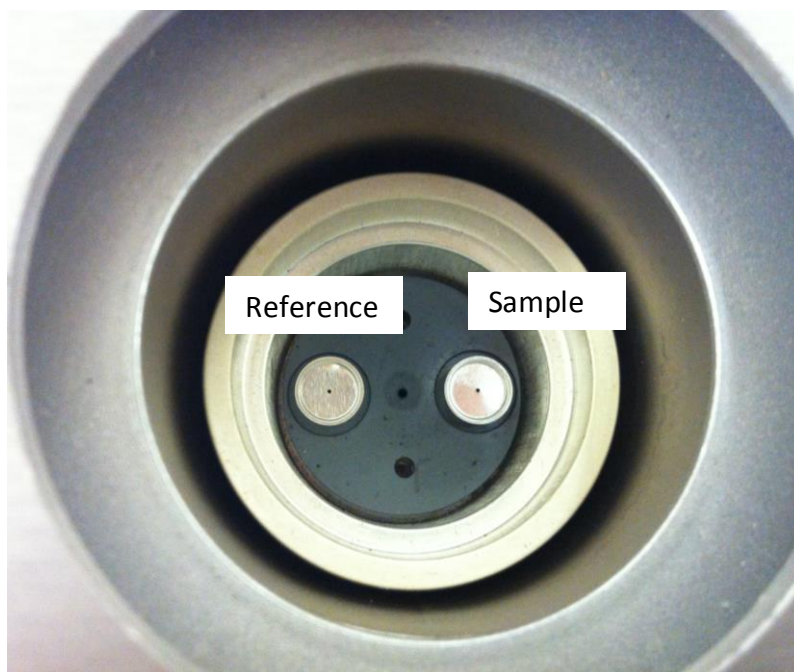


Figure 4.7 Pans and the inside of the DSC Device

After the baseline test was done. The sample crucible on the right was taken and the reference material, Al_2O_3 Sapphire was put and the crucible placed back into the equipment. The sapphire was replaced with the IM7-G/8552 Unidirectional composite material to measure the heat flux in respect to the temperature. Measurement of the composite material was done at the last step. Then, the specific heat capacity could be calculated by using the ratio method. Figure 4.8 shows the reference material (sapphire) and the IM7-G/8552 with pans and lids.



Figure 4.8 The Sapphire and IM7-G/8552 with pans and lids

Table 4.10

The measured specific heat data of IM7-G/8552

Temp, °C	Specific Heat, Cp, J/g°C					STD	% CV
	S-Cp-1	S-Cp-2	S-Cp-3	S-Cp-4	Average		
22	0.8809	0.9294	0.8972	0.9099	0.9043	0.0205	2.3
29	0.9229	0.9638	0.9342	0.9493	0.9425	0.0178	1.9
38	0.9725	1.0115	0.9791	0.9955	0.9896	0.0175	1.8
46	1.0109	1.0575	1.0170	1.0325	1.0295	0.0208	2.0
57	1.0617	1.1152	1.0683	1.0808	1.0815	0.0238	2.2
68	1.1145	1.1653	1.1212	1.1309	1.1330	0.0226	2.0
78	1.1550	1.2050	1.1628	1.1768	1.1749	0.0220	1.9
89	1.1921	1.2449	1.2035	1.2169	1.2143	0.0228	1.9
99	1.2278	1.2819	1.2400	1.2519	1.2504	0.0232	1.9

The specific heat measurements of the four samples of IM7-G/8552 unidirectional composites all show trends that are extremely close to linear. The tests were run from 22°C to 99°C. All specimens were tested at same temperature program. The comparison of the results can be found in Table 4.10. The average and the standard deviation of the four specimens are listed in last two columns. Figure 4.9 illustrates plot of the C_p versus temperature for all four specimens. The specific heat of the materials increased as the testing temperature increases. This was expected since the molecules energy increase with the temperature. The equation of the average values of C_p obtained by the least square regression which is followed by:

$$C_p = 0.816 + 4.5 \times 10^{-3} T \quad (4.7)$$

With the R value of 0.99.

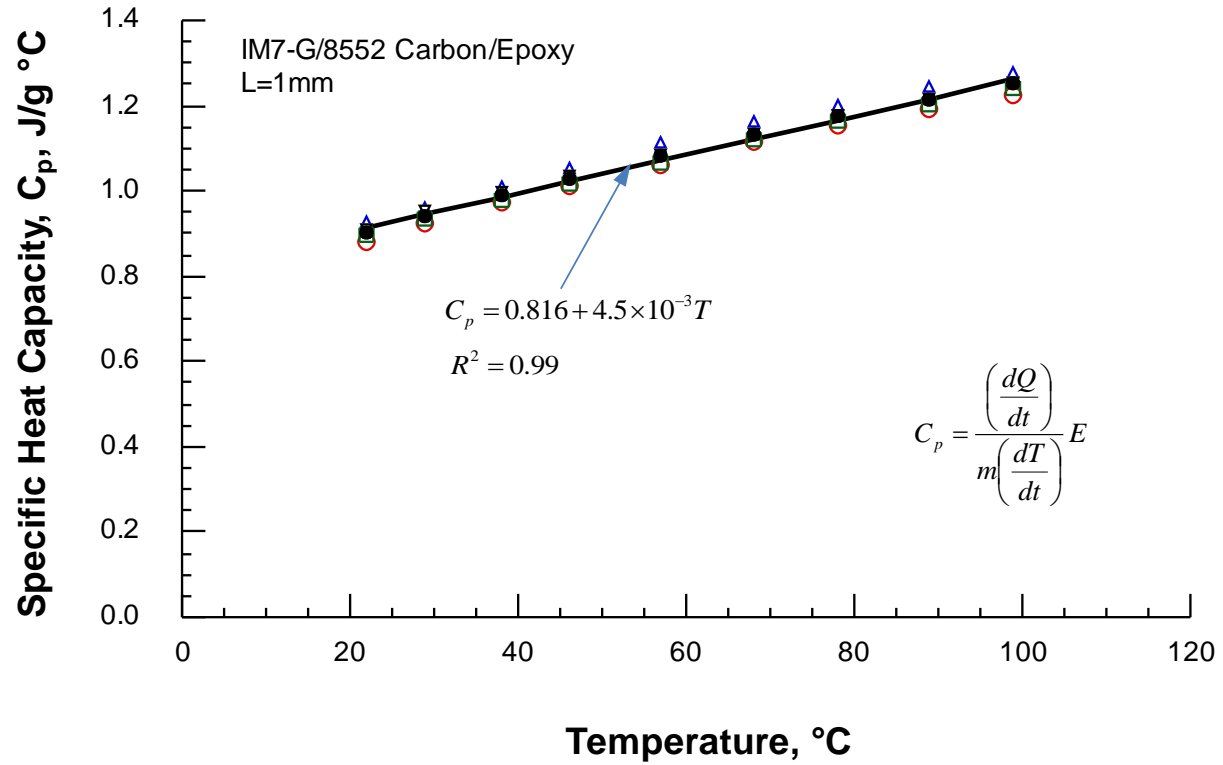


Figure 4.9 The specific heat measurement of the IM7-G/8552

The error calculation of specific heat capacity was made. To make calculation, standard deviation, standard error determined, and then percent error was calculated with using average values of C_p at each temperature. The Error data is given in table 4.11 and the graph is given by Figure 4.10.

Table 4.11

The Percent Error of Specific Heat Capacity

Temp, T °C	Average, cm ² /s	STD	<i>e</i>	Percent error
22	0.9043	0.0205	0.0180	2.0
29	0.9425	0.0178	0.0156	1.7
38	0.9896	0.0175	0.0153	1.5
46	1.0295	0.0208	0.0182	1.8
57	1.0815	0.0238	0.0209	1.9
68	1.1330	0.0226	0.0198	1.7
78	1.1749	0.0220	0.0193	1.6
89	1.2143	0.0228	0.0199	1.6
99	1.2504	0.0232	0.0203	1.6

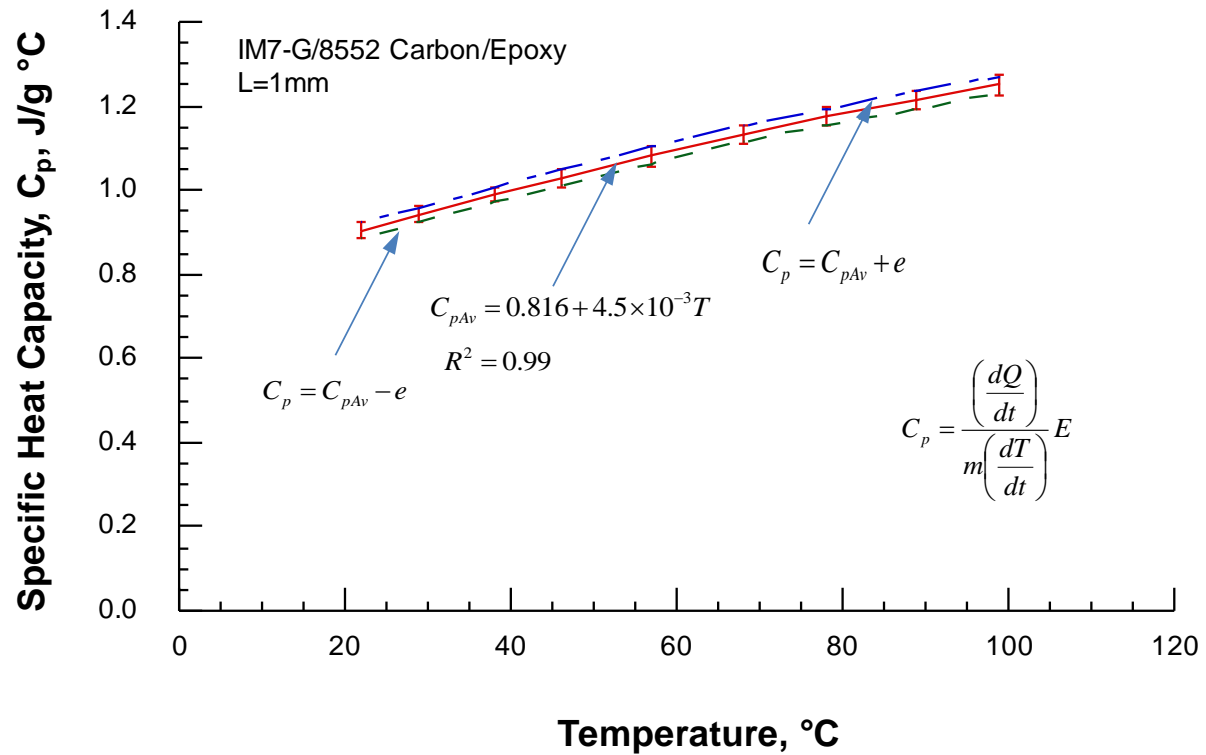


Figure 4.10 Error diagram of the specific heat C_p of IM7/8552

4.4 Thermal Conductivity

The density, specific heat, and thermal diffusivity were used to determine the thermal conductivity of IM7-G/8552 unidirectional composite material by using the following equation:

$$k = \rho \times C_p \times \alpha \quad (4.8)$$

The thermal diffusivity and specific heat capacity are explained in detailed in previous chapters. In addition, the measurement results are presented in this chapter. The density is calculated with using the equation:

$$\rho = \frac{m}{V} \quad (4.9)$$

Mass, m , is measured with Mettler Toledo XP6 weighing equipment which is able to give 6 decimal of gram. Then, volume was calculated by measuring the diameter and the thickness of the each specimen. The calculated average density (ρ) of the laminate was 1.57 g/cm^3 . The results for the thermal conductivity of IM7-G/8552 in axial and transverse direction are shown in Table 4.12 and 4.13.

Table 4.12

Thermal Conductivity of IM7-G/8552 in axial direction, k_1

Temp, T °C	Conductivity k_1 , w/m°C, $\rho = 1.57 \text{ g/cm}^3$						STD	%CV
	S-A-1	S-A-2	S-A-3	S-A-4	S-A-5	Average		
22	4.8960	4.9244	4.8675	4.8960	4.9102	4.8988	0.0211	0.4
29	5.2067	5.1474	5.1326	5.0287	5.1326	5.1296	0.0641	1.3
38	5.3890	5.3734	5.3578	5.2800	5.3890	5.3578	0.0454	0.8
46	5.5087	5.5411	5.5897	5.4439	5.5411	5.5249	0.0537	1.0
57	5.7701	5.7701	5.8212	5.6510	5.7701	5.7565	0.0630	1.1
68	5.9913	6.0091	6.0626	5.9556	6.0983	6.0234	0.0569	0.9
78	6.1575	6.2315	6.3424	6.1945	6.3609	6.2573	0.0902	1.4
89	6.3641	6.4215	6.5170	6.5361	6.1921	6.4062	0.1387	2.2
99	6.4941	6.6122	6.9271	6.4941	6.6516	6.6358	0.1773	2.7

Table 4.13

Thermal Conductivity of IM7-G/8552 in transverse direction, k_3

Temp, T °C	Conductivity k_3 , w/m°C, $\rho = 1.57 \text{ g/cm}^3$						%CV
	S-T-1	S-T-2	S-T-3	S-T-4	Average	STD	
22	0.5835	0.5408	0.5835	0.6262	0.5835	0.0349	6.0
29	0.6082	0.5637	0.5785	0.6379	0.5971	0.0329	5.5
38	0.6230	0.5919	0.5919	0.6697	0.6191	0.0368	5.9
46	0.6481	0.5995	0.6157	0.6805	0.6359	0.0359	5.6
57	0.6638	0.6298	0.6468	0.7149	0.6638	0.0368	5.5
68	0.6954	0.6419	0.6776	0.7489	0.6910	0.0446	6.5
78	0.7027	0.6657	0.7027	0.7581	0.7073	0.0381	5.4
89	0.7262	0.6880	0.7071	0.7836	0.7262	0.0413	5.7
99	0.7478	0.7085	0.7085	0.8068	0.7429	0.0465	6.3

The thermal conductivity of the axial direction is much higher than that of transverse direction. The magnitude of highness is almost 10 times because the heat is able to transfer longitudinally along the fiber better than the across the fiber. Furthermore, the heat must transit

across the resin that has less conductivity than carbon fiber. This causes the lower thermal conductivity in transverse direction. The figure 4.11 and 4.12 shows the results of transverse and longitudinal results of IM7-G/8552. The equation of the average values of k_l obtained by the least square regression which is followed by:

$$k_l = 4.49 + 2.25 \times 10^{-2} T \quad (4.10)$$

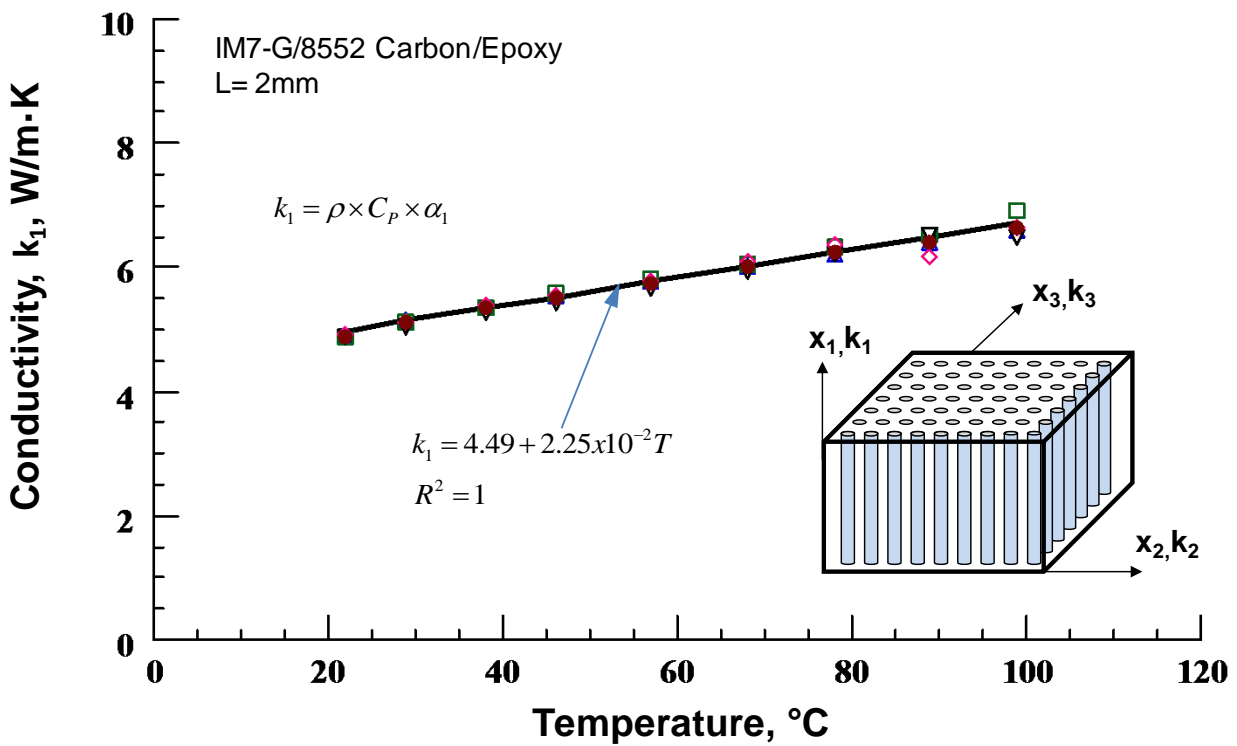


Figure 4.11 Thermal Conductivity of IM7-G/8552 in longitudinal direction

Five samples of transverse conductivity measurements are constant and close to linear. Mean equation is given in the graph. The equation of the average values of k_3 obtained by the least square regression which is followed by:

$$k_3 = 0.548 + 2.1 \times 10^{-3} T \quad (4.11)$$

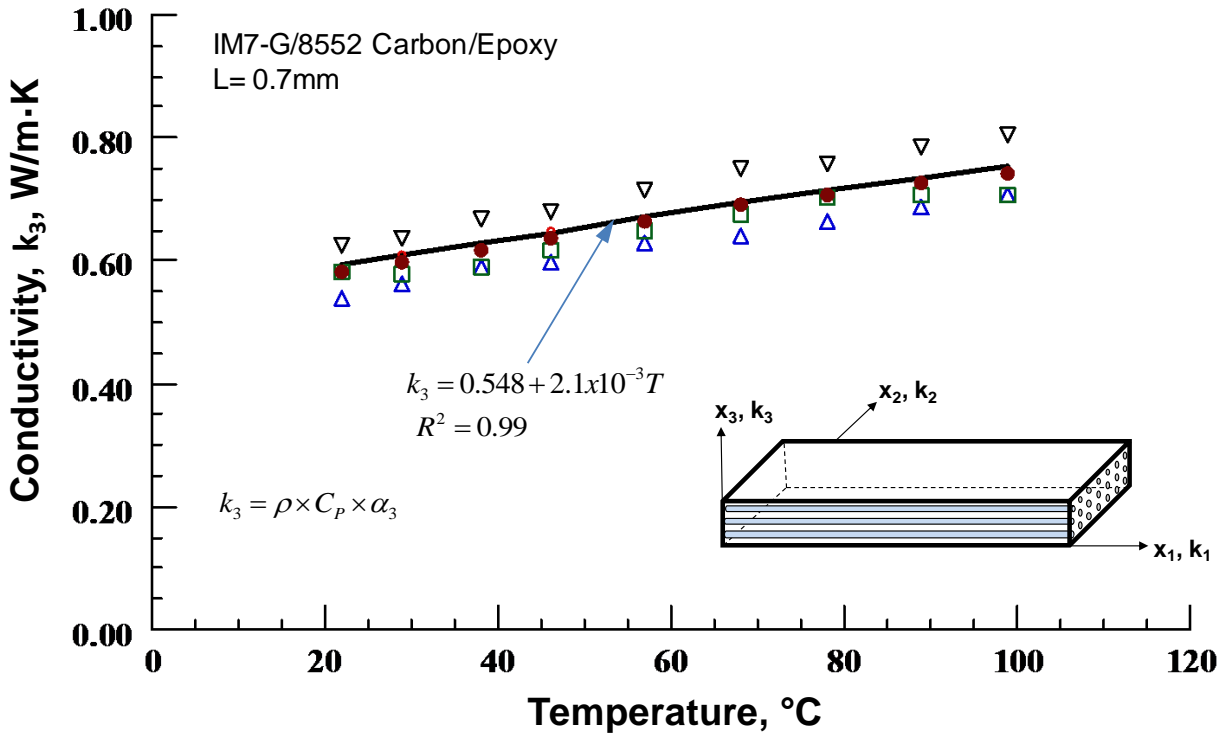


Figure 4.12 Thermal Conductivity of IM7-G/8552 in transverse direction

The five samples of longitudinal thermal conductivity results are given in the diagram. The results show that transverse thermal conductivity of IM7-G/8552 is approximately 10 times higher than the longitudinal thermal conductivity. This is expected since the heat does not cross the resin that has much lower thermal conductivity and heat transfer through the thickness is lower from the longitudinal.

4.5 Special Studies

Two special studies were performed in this research. The first study was independency of specific heat with specimen geometry, keeping the mass same. The second study was the effect of surface coating on thermal diffusivity on carbon/epoxy composite specimen.

4.5.1 Specimen shape effect on specific heat capacity. Although it was believed that the specific heat is a material property and independent of geometry, it was reevaluated for

carbon/epoxy composites. Three different shapes of composite material were cut, namely square, rectangular, and circular shapes specimen geometry were presented in chapter 3. These three types of specimens were tested in NETZSCH DSC equipment and measured C_p with temperature are listed in tables of 4.14 through 4.17.

Table 4.14

Specific heat capacity of IM7-G/8552-1 square shape samples

Temp, °C	Specific Heat, C_p, J/g°C				
	S-Sq-1	S-Sq-2	S-Sq-3	S-Sq-4	Average
20	0.8557	0.8212	0.8901	0.9083	0.8688
30	0.8976	0.8642	0.9377	0.9468	0.9116
40	0.9315	0.8988	0.9748	0.9798	0.9462
50	0.9638	0.9365	1.0145	1.0093	0.9810
60	0.9948	0.9729	1.0500	1.0385	1.0140
70	1.0261	1.0084	1.0851	1.0668	1.0466
80	1.0553	1.0412	1.1173	1.0949	1.0772
90	1.0862	1.0730	1.1489	1.1226	1.1077
100	1.1166	1.1037	1.1792	1.1513	1.1377

Table 4.15

Specific heat capacity of IM7-G/8552-1 circular shape samples

Temp, °C	Specific Heat, Cp, J/g°C				Average
	S-Cr-1		S-Cr-2		
	1st Run	2nd Run	1st Run	2nd Run	
20	0.8895	0.9327	0.91905	0.84185745	0.8958
30	0.9231	0.9606	0.9495	0.9319	0.9413
40	0.9578	0.9959	0.9819	0.9663	0.9755
50	0.9924	1.0265	1.0189	0.9979	1.0089
60	1.0262	1.0572	1.0552	1.0294	1.0420
70	1.0589	1.0872	1.0884	1.0606	1.0737
80	1.0911	1.1161	1.1197	1.0905	1.1043
90	1.1234	1.1455	1.1494	1.1207	1.1347
100	1.1554	1.1750	1.1777	1.1511	1.1648

Table 4.16

Specific heat capacity of IM7-G/8552-1 rectangular shape samples

Temp, °C	Specific Heat, Cp, J/g°C					Average
	S-Re-1	S-Re-2	S-Re-3	S-Re-4	S-Re-5	
20	0.9347	0.9408	0.8494	0.8755	0.9590	0.9119
30	0.9723	0.9709	0.8860	0.9147	0.9951	0.9478
40	1.0049	0.9989	0.9197	0.9489	1.0241	0.9793
50	1.0358	1.0257	0.9529	0.9852	1.0537	1.0107
60	1.0636	1.0531	0.9842	1.0185	1.0823	1.0403
70	1.0922	1.0802	1.0158	1.0523	1.1140	1.0709
80	1.1200	1.1074	1.0464	1.0823	1.1443	1.1001
90	1.1474	1.1335	1.0771	1.1107	1.1746	1.1287
100	1.1753	1.1605	1.1082	1.1375	1.2052	1.1574

Table 4.17

Comparison of specific heat capacity of IM7-G/8552-1 samples

Temp, °C	Specific Heat, Cp, J/g°C				
	S-Re	S-Cr	S-Sq	Variation (Cir/Rec)	Variation (Sq/Cir)
20	0.8688	0.8958	0.9119	9.7397	1.7644
30	0.9116	0.9413	0.9478	2.9907	0.6865
40	0.9462	0.9755	0.9793	2.9762	0.3923
50	0.9810	1.0089	1.0107	2.7939	0.1731
60	1.0140	1.0420	1.0403	2.6343	-0.1576
70	1.0466	1.0737	1.0709	2.4467	-0.2645
80	1.0772	1.1043	1.1001	2.2973	-0.3867
90	1.1077	1.1347	1.1287	2.1606	-0.5402
100	1.1377	1.1648	1.1574	2.0350	-0.6422

In all three cases C_p variation is with 3% and over the temperature range 20 to 100°C. These results reconfirm the independency of the specific heat with the specimen shape as long as the specimen mass is small and specimen maintains uniform temperature at each measurement. The figure 4.x shows the plot C_p vs T for three different shapes. The results follow the linear equation:

$$C_p = 0.836 + 3.2 \times 10^{-3} T \quad (4.12)$$

With the R value of 0.99.

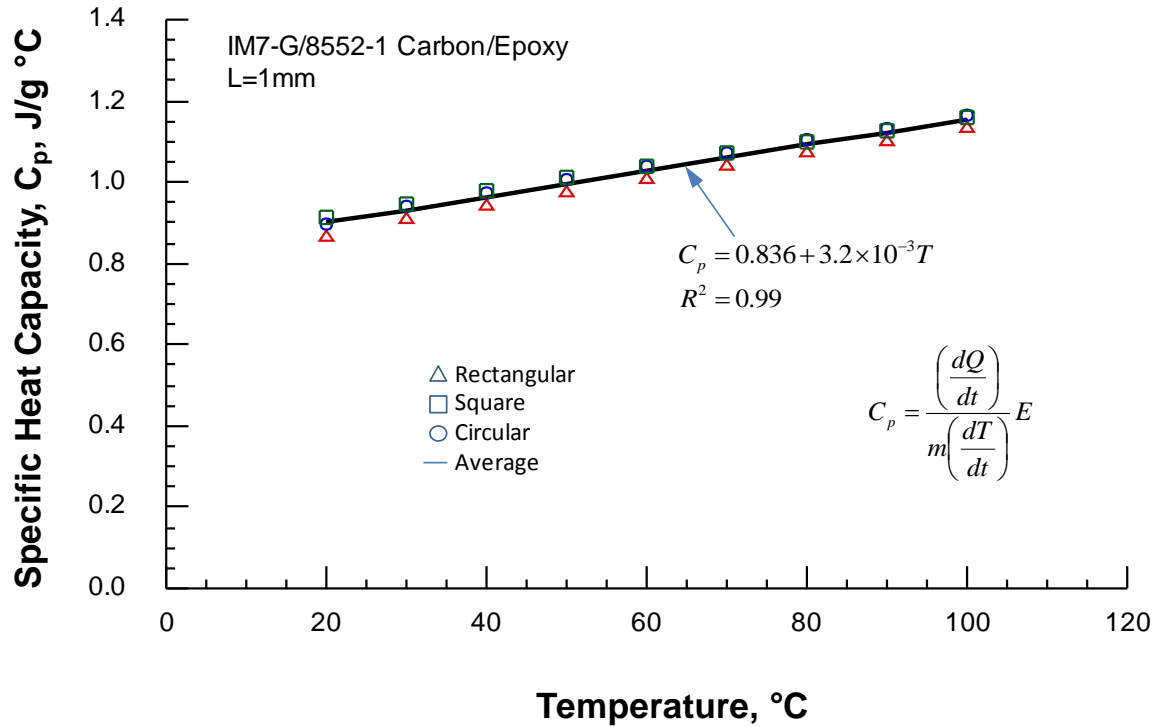


Figure 4.13 Specific Heat capacity versus temperature for three of different shapes of specimens

4.5.2 Effect of surface coating on thermal diffusivity. In this test, the effect of carbon coating on the specimen top and bottom surfaces on the thermal diffusivity of the carbon/epoxy composite was assessed. One sample of the axial thermal diffusivity and one sample through the thickness (transverse) thermal diffusivity were chosen, coated. Specimen diffusivity was measured before and after graphite powder. The two results for temperature range of 20 to 100°C are listed in table 4.18 and the sample results are compared in Figure 4.14 and 4.15, respectively for axial and transverse directions. The percent difference between coated and uncoated varied from 1.74% to 2.7% in axial direction and between 0 and 2.3% in transverse direction. The difference is generally at high temperature but still less than 3%. Therefore, graphite powder coating had no effect on the measurement.

Table 4.18

Thermal Diffusivity comparison of coated and plain samples in two directions

Temp, T °C	Diffusivity, α_1 , cm ² /s, L=1.98mm			%CV	Diffusivity, α_1 , cm ² /s, L=0.63mm		
	Original	Coated			Original	Coated	%CV
20	0.0344	0.0350		1.7	0.0041	0.0041	0.0
29	0.0351	0.0348		-0.9	0.0041	0.0041	0.0
38	0.0346	0.0341		-1.4	0.0040	0.0040	0.0
46	0.0340	0.0342		0.6	0.0040	0.0040	0.0
57	0.0339	0.0342		0.9	0.0039	0.0039	0.0
67	0.0336	0.0337		0.3	0.0039	0.0039	0.0
78	0.0333	0.0334		0.3	0.0038	0.0039	2.6
89	0.0333	0.0342		2.7	0.0038	0.0038	0.0

Thermal diffusivity of carbon graphite coated and plain composite specimens are in axial and transverse directions in figure 4.2 and 4.3.

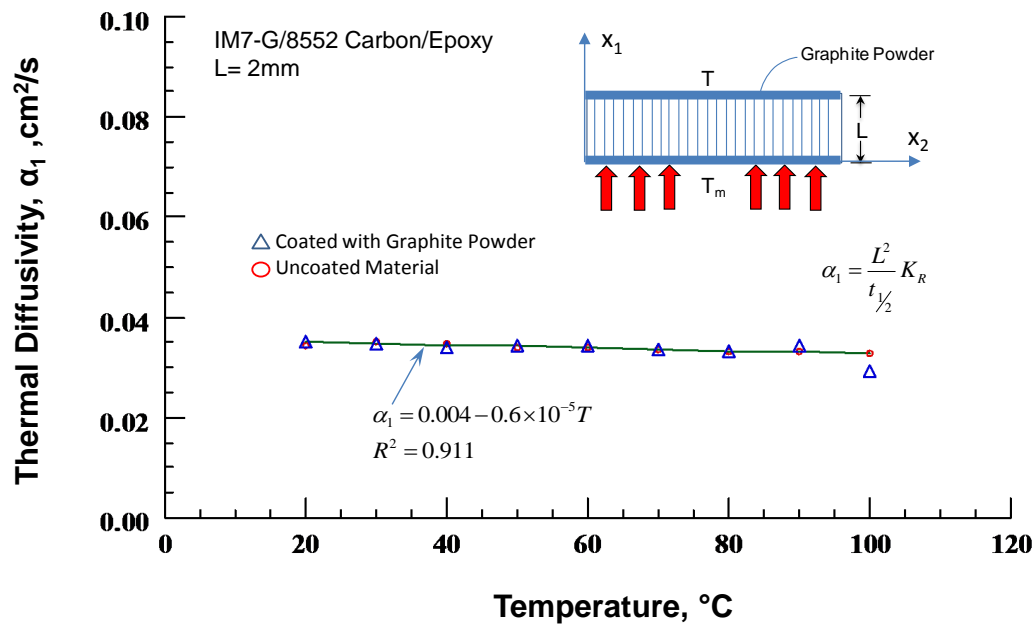


Figure 4.14 Thermal Diffusivity comparison of carbon coated and uncoated materials in axial direction

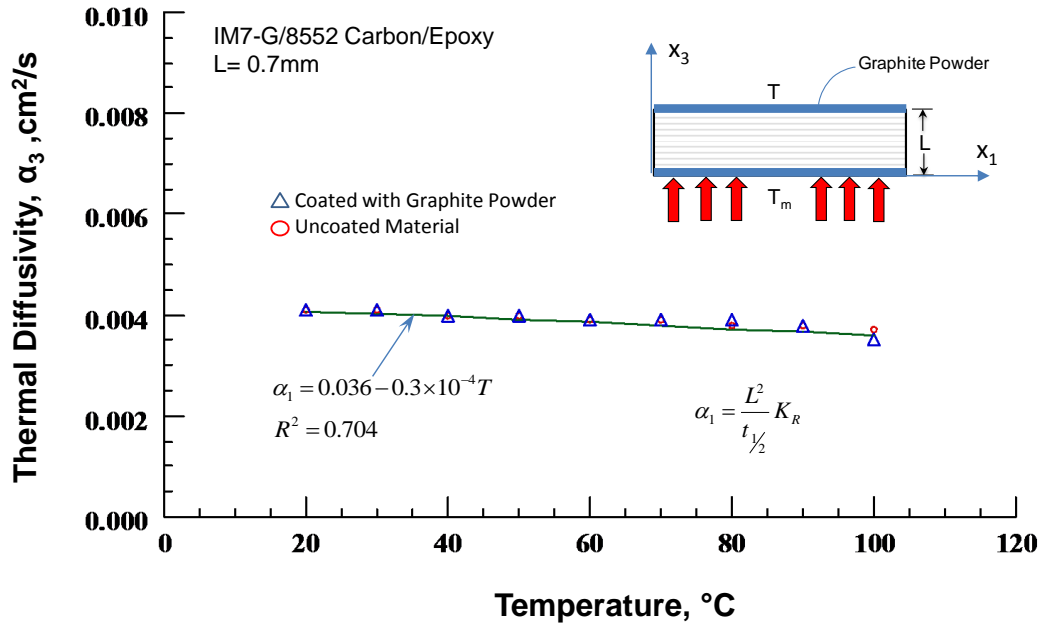


Figure 4.15 Thermal Diffusivity comparison of carbon coated and uncoated materials in transverse direction

As a result, when we compared the data, there is no effect of graphite powder to the thermal diffusivity of the materials since the diffusivity variations are under 3%, at most of the segments under 1%. Graphite powder does not affect the thermal diffusivity.

4.6 Summary

Anter Flashline 2000 was used to measure thermal diffusivity and NETZSCH DSC 200 F3 Maia was used to measure specific heat capacity of IM7-G/8552. Thermal diffusivity was measured in two different directions by Anter Flashline. Specimens were prepared by axial and transverse direction of the fiber to get both axial and transverse thermal diffusivity and conductivity of the composite material. Test results were presented in this chapter. The following equations are obtained for axial and transverse directions.

$$C_p = 0.816 + 4.5 \times 10^{-3} T \quad (4.12)$$

$$\alpha_1 = 0.035 - 1 \times 10^{-5} T \quad (4.13)$$

$$\alpha_3 = 0.0042 - 4 \times 10^{-5} T \quad (4.14)$$

Then, thermal conductivity equations obtained as:

$$k_1 = 4.49 + 2.25 \times 10^{-2} T \quad (4.15)$$

$$k_3 = 0.548 + 2.1 \times 10^{-3} T \quad (4.16)$$

All the equations were developed for a temperature range 22°C to 100°C. However, extension of the equations from 0°C to 125°C will give reasonable accurate results.

The thermal conductivity of IM7-G/8552 composite laminate at room temperature is $k_1 = 4.89$ W/m°C and $k_3 = k_2$ since the transverse isotropy of the unidirectional composite material $k_3 = 0.58$ W/m°C. Thermal diffusivity results in both directions at room temperature are $\alpha_1 = 0.034$ cm²/s and $\alpha_3 = 0.0041$ cm²/s. Specific heat capacity of IM7-G/8552 is $C_p = 0.904$ J/g°C at room temperature (22°C).

The conductivity of similar composites, such as AS4/3501-6 Carbon/Epoxy is $k_1 = 4.9$ W/m°C and $k_3 = 0.69$ W/m°C with thermal diffusivity of AS4/3501-6 is $\alpha_1 = 0.039$ cm²/s and $\alpha_3 = 0.0054$ cm²/s, and the specific heat capacity is $C_p = 0.898$ J/g°C at room temperature (22°C) (Osman, 2015).

CHAPTER 5

Thermal Conductivity of Fiber Reinforced Composites by Micromechanics

5.1 Introduction

This chapter describes prediction of axial and transverse thermal conductivity of the unidirectional IM7-G/8552 composites by micromechanics analysis. Rule of mixture was used to calculate longitudinal (k_l) and six models from literature were used to calculate transverse thermal conductivity (k_t) of the composite. The predicted values were compared with the experimental data in chapter 4.

5.2 Unit Cell Model

The unit cell model shown in the figure 5.1 explains an idealized structure of the unidirectional fiber reinforced composite material. The unit cube cell model describes that the fiber is distributed in a square array. The rule of mixture was successfully used in Springer and Tsai (1967) to calculate k_l . There are number of models in literature for transverse conductivity based different assumptions, among than six are presented here.

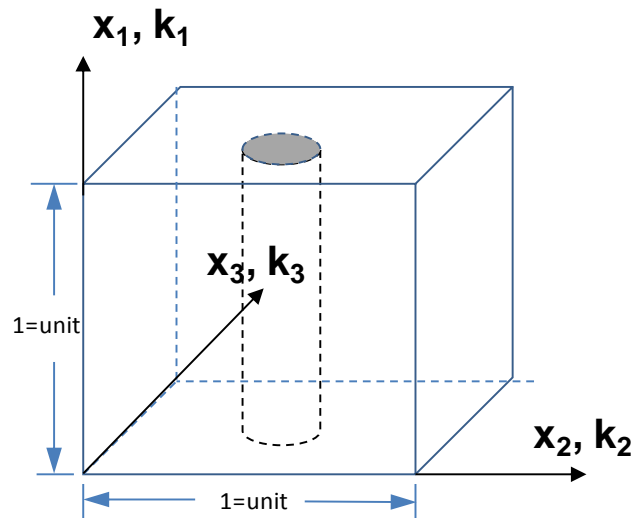


Figure 5.1 Unit cell of a unidirectional composite laminate

5.2.1 Axial conductivity (k_l) models. The resin is assumed as isotropic and the fiber is orthotropic. Springer and Tsai (1967) and Thornburgh and Pears (1965) proposed rule of mixture model to calculate axial thermal conductivity of the composite by the equation:

$$k_l = V_f k_{lf} + V_m k_m \quad (5.1)$$

Where k_l is the composite axial thermal conductivity, V_f is the fiber volume fraction, k_{lf} is the longitudinal thermal conductivity of the fiber, k_m is the thermal conductivity of the matrix, and the matrix volume fraction is $V_m = 1 - V_f$. IM7 fiber and 8552 matrix conductivity properties were taken from Hexcel Tow[®] IM7 Product Data Sheet and Johnston (1997). Using these values and measured $V_f = 0.58$ the k_l of the composite was calculated using equation 5.1 and it was found to be 3.19 W/m°C. However, the measured k_l was 4.9 W/m°C. As explained in the literature, the equation 5.1 is suppose to accurately predicts k_l therefore fiber k_{lf} was back calculated for $k_l = 4.9$ W/m°C agrees with the measured k_l . The resulting k_{lf} is 8.34 W/m°C, and this is also listed in table 5.1 within parenthesis.

Table 5.1

Constituent thermal conductivity

Materials	V_f	Conductivity, W/m°C			
		Fiber, k_f	Matrix, k_m	Equation 5.1, k_l	Present Experiment, k_l
IM7-G/8552	0.58	5.4 ¹ (8.34) ²	0.148 ³	3.19	4.9
AS Graphite/Epoxy ⁴	0.60	5.22	0.190	-	-

¹ Hexcel Tow[®] IM7 Product Data

² Back calculated value by rule of mixture, Equation 5.1

³ Johnston (1997)

⁴ Wetherhold and Wang (1994)

5.2.2 Transverse conductivity (k_3) models. Prediction of through the thickness thermal conductivity (k_3) is more complex than axial conductivity. There are number of analytical models reported in the literature for calculation of k_3 . Commonly used six models are reviewed in and are summarized below. The following six models are validated by (Wetherhold & Wang, 1994), for AS Graphite Epoxy composite. Constituent properties of the material are listed in table 5.1.

1. Rayleigh (1892): Rayleigh used the analogy of obstacles arranged in rectangular to derive the equation.

$$k_3 \approx k_m \left(1 - \frac{2V_f}{v' + V_f - \frac{C_1}{v'} V_f^4 - \frac{C_2}{v'} V_f^8} \right)$$

$$C_1 = 0.3058$$

$$C_2 = 0.0134$$

$$v' = \frac{\left(\frac{k_m}{k_f + 1} \right)}{\left(\frac{k_m}{k_f - 1} \right)}$$
(5.2)

2. Halphin and Tsai (1964): Halphin – Tsai model is based on bounding principles and analogies to mechanical (shear) properties.

$$k_3 = k_m \left[\frac{1 + \xi \eta v_f}{1 - \eta v_f} \right]$$

$$\eta = \frac{\left(\frac{k_f}{k_m} \right) - 1}{\left(\frac{k_f}{k_m} \right) + \xi}$$

$$\xi = 1$$
(5.3)

4. Hashin (1983): Hashin model is based on bounding principles and analogies to mechanical (shear) properties. This model is same as Halpin-Tsai equation, except it is written in the different form.

$$k_3 = k_m + \frac{V_f}{\frac{1}{k_f - k_m} + \frac{1 - V_f}{2k_m}} \quad (5.4)$$

3. Springer and Tsai (1967): Springer – Tsai is based on simple combinations of thermal resistance model

$$k_3 = k_m \left[\left(1 - 2\sqrt{\frac{V_f}{\pi}} \right) + \frac{1}{B} \left[\pi - \frac{4}{\sqrt{1 - \left(\frac{B^2 V_f}{\pi} \right)}} \tan^{-1} \frac{\sqrt{1 - \left(\frac{B^2 V_f}{\pi} \right)}}{1 + B\sqrt{\frac{V_f}{\pi}}} \right] \right] \quad (5.5)$$

$$B = 2 \left(\frac{k_m}{k_f} - 1 \right)$$

5. Chawla (2012): Chawla is based on simple combinations of thermal resistance model.

$$k_3 = k_m \left(\left(1 - \sqrt{V_f} \right) + \frac{\sqrt{V_f}}{1 - \sqrt{V_f} \left(1 - \frac{k_m}{k_f} \right)} \right) \quad (5.6)$$

6. Farmer and Covert (1994):

$$k_3 \approx k_m \left(1 - \frac{2V_f}{v' + V_f - \frac{C_1}{v'} V_f^4 - \frac{C_2}{v'} V_f^8} \right) \quad (5.7)$$

$$C_1 = 0.3058 \text{ and } C_2 = 0.0134$$

$$v' = \frac{\frac{k_m}{k_f} + 1 + \frac{k_m}{ah_c}}{\frac{k_m}{k_f} - 1 + \frac{k_m}{ah_c}}$$

Rayleigh and Farmer-Covert models are the same except for interphasial property effect. If the interphasial effect is neglected the two models give the same results, which is the case in present analysis. Therefore, the model was not used because α and h_c are not known.

The k_3 was calculated using all models for AS Graphite/ Epoxy composite using the constituent properties given in Table 5.1. The resulting k_3 is compared with literature data (Wetherhold & Wang, 1994) $k_3 = 0.71$ W/mK and found at Rayleigh's model agrees very well while all other models gave about 7% less.

Table 5.2

Comparison of predicted k_3 of AS Graphite/Epoxy composite with the literature data

Models	Calculated k_3 , W/mK
Rayleigh	0.710
Halpin-Tsai	0.669
Springer-Tsai	0.655
Chawla	0.657
Literature ¹	0.710

¹ $k_3 = 0.71$ W/mK (Wetherhold & Wang, 1994)

5.2.3 Comparison of predicted k_3 with experimental data. Table 5.3 lists the k_3 calculated from Equation 5.2, through 5.4, and 5.6 for $V_f=0.58$. Among the four models, Rayleigh's model predicts (0.554 W/m°C) the closest results to the experimental data (0.584 W/m°C) for $k_f = 8.34$ W/m°C. The difference is about 5%. All other models predicts lower values, Chawla's model predicts the lowest. Since the conductivity k_3 is sensitive to V_f , k_3 was calculated and listed for $V_f=0.57$ and 0.59 (0.01 on either side of the V_f) and the deviation is about 0.02 W/m°C. The difference between Rayleigh's model and experiment reduced to 2% for $V_f=0.59$.

Table 5.3

Comparison of predicted and measured conductivity k_3 of IM7-G/8552

Model	Calculated Conductivity k_3 , W/m°C				Measured k_3
	$V_f=0.58,$ $k_f=5.4$ W/m°C	$k_f=8.34$ W/m°C			
		$V_f=0.58$	$V_f=0.57$	$V_f=0.59,$	
Rayleigh	0.535	0.554	0.536	0.574	0.584
Halpin-Tsai	0.508	0.524	0.510	0.539	
Springer-Tsai	0.491	0.508	0.490	0.527	
Chawla	0.488	0.495	0.480	0.510	
Farmer-Covert	0.535	0.554	0.536	0.574	

Predicted value of k_3 using the Hexcel data sheet $k_f=5.4$ W/m°C is also listed in table 5.3 and it is 0.535 W/m°C based on Raleigh's model. This value is much lower than estimated $k_f=8.34$ W/m°C.

5.3 Summary

The rule of mixture is accurate for prediction of k_l , providing the fiber axial conductivity is accurate. However, Halphin-Tsai, Springer-Tsai, and Chawla models gave nearly same value of k_3 but 11-16% lower than the experiment. Rayleigh's model predicted 5-11% higher than Halphin-Tsai, Springer-Tsai, and Chawla models and 5% lower than measured value ($k_3 = 0.584$ W/m°C)

CHAPTER 6

Concluding Remarks and Future Work

6.1 Concluding Remarks

Thermal conductivity of IM7-G/8552 fiber reinforced composite laminate was determined using measured thermal diffusivity (α), specific heat capacity (C_p), and material density (ρ). Then the conductivity was calculated from the equation:

$$k = \alpha \times C_p \times \rho \quad (6.1)$$

This approach is commonly used for isotropic materials and the approach is standardized by ASTM E-1461 and ASTM E-1269. Here this approach was applied to unidirectional composite laminate to determine both axial and transverse thermal conductivity. The novelty of the approach is in the specimen preparation to adapt the existing simple and accurate technique to determine both axial and transverse conductivity of a unidirectional composite.

Anter Flashline was used to measure thermal diffusivity for along and across fiber direction of the unidirectional fiber composite. Because the transverse plane (x_2 - x_3) is isotropic, thermal diffusivity in x_1 (α_1) and x_3 (α_3) directions are only parameters needed. Two types of cylindrical specimens with diameter 12.5 mm were prepared to measure axial and transverse thermal diffusivities. The reinforcing fibers are along and across the heat flow directions in the axial and transverse test specimen, respectively.

Small size of specimens (11.5 mg) were prepared to maintain constant temperature on samples to measure specific heat capacity (C_p). Thermal diffusivity and specific heat capacity were measured for a temperature range 20°C to 100°C and at least for four specimen for each test case. Using the measured diffusivity, specific heat capacity at each temperature, and the density of the specimen the conductivity was calculated.

The average thermal diffusivity along the fiber of IM7-G/8552 composite laminate was found to be:

$$\alpha_1 = 0.035 - 1 \times 10^{-5} T \quad (6.2)$$

Thermal diffusivity across the fiber,

$$\alpha_3 = 0.0042 - 4 \times 10^{-5} T \quad (6.3)$$

The specific heat of the composite is,

$$Cp = 0.816 + 4.5 \times 10^{-3} T \quad (6.4)$$

The average densities (ρ) of the axial and transverse specimens were 1.58 and 1.57 g/cm³, respectively. The calculated thermal conductivity in axial (k_1) and transverse (k_3) followed the equations,

$$k_1 = 4.49 + 2.25 \times 10^{-2} T \quad (6.5)$$

$$k_3 = 0.548 + 2.1 \times 10^{-3} T \quad (6.6)$$

The parameter T is the temperature in Celsius. Thermal diffusivity is nearly constant or shows small decreases with temperature. However, specific heat capacity and thermal conductivity increased with temperature rise. The room temperature conductivity of IM7-G/8552 composite laminate are $k_1 = 4.89$ W/m°C and $k_3 = 0.58$ W/m°C. Because of nonavailability of IM7-G/8552 data, the measured conductivities are compared with similar composites and the micromechanics prediction in the literature. The conductivity of AS4/3501-6 carbon/epoxy $k_3 = 0.61$ W/m°C and prediction of $k_3 = 0.55$ W/m°C at room temperature (Saad & Doleman, 2013). The equations 6.5 and 6.6 are valid for temperature between 20°C and 100°C.

6.2 Future Work

Based on the research performed in this thesis following future work are suggested.

1. Extended work to characterize the thermal conductivities of composite at cryogenic temperatures for space applications.
2. Measure multidirectional conductivity of a composite laminate and validate by the macromechanics models.
3. Extend the work to measure electrical and magnetic properties of composite laminate.

References

- Anter Corporation. FlashLine™ Thermal Diffusivity Measuring System Operation and Maintenance Manual Part 1 Flashline 2000.
- ASTM Standard C-1113. (2005). Standard Test Method for Thermal Conductivity of Refractoriess by Hot Wire (Platinum Resistance Thermometer Technique). West Conshohocken, PA: ASTM International.
- ASTM Standard E-1269. (2005). Standard Test Method for Determining Specific Heat Capacity by Differential Scanning Calorimetry. West Conshohocken, PA: ASTM International.
- ASTM Standard E-1461. (2007). Standard Test Method for Thermal Diffusivity by the Flash Method. West Conshohocken, PA: ASTM International.
- Behzad, T, & Sain, M. (2007). Measurement and prediction of thermal conductivity for hemp fiber reinforced composites. *Polymer Engineering & Science*, 47(7), 977-983.
- Blumm, J, & Kaisersberger, E. (2001). Accurate measurement of transformation energetics and specific heat by DSC in the high-temperature region. *Journal of thermal analysis and calorimetry*, 64(1), 385-391.
- Cernuschi, F, Bison, PG, Marinetti, S, Figari, A, Lorenzoni, L, & Grinzato, E. (2002). Comparison of thermal diffusivity measurement techniques. *Quantitative InfraRed Thermography Journal*.
- Chawla, Krishan K. (2012). *Composite materials: science and engineering*: Springer Science & Business Media.
- Clark III, LM, & Taylor, RE. (1975). Radiation loss in the flash method for thermal diffusivity. *Journal of Applied Physics*, 46(2), 714-719.

- Coquard, R, & Panel, B. (2009). Adaptation of the FLASH method to the measurement of the thermal conductivity of liquids or pasty materials. *International Journal of Thermal Sciences*, 48(4), 747-760.
- Cowan, Robert D. (1963). Pulse method of measuring thermal diffusivity at high temperatures. *Journal of Applied Physics*, 34(4), 926-927.
- Daniel, Isaac M, & Ishai, Ori. (1994). *Engineering mechanics of composite materials* (Vol. 3): Oxford university press New York.
- Ditmars, David A, & Douglas, Thomas B. (1971). Measurement of the relative enthalpy of pure e-A120 3 (NBS heat capacity and enthalpy standard reference material no. 720) from 273 to 1,173 K. *J Res Nat Bur Stand A*, 75, 401-420.
- Farmer, Jeffrey D, & Covert, Eugene E. (1994). Transverse thermal conductance of thermosetting composite materials during their cure. *Journal of thermophysics and heat transfer*, 8(2), 358-365.
- Figliola, Richard S, & Beasley, Donald. (2011). *Theory and design for mechanical measurements*: John Wiley & Sons.
- Halpin, JC, & Kardos, JL. (1976). The Halpin-Tsai equations: a review. *Polymer Engineering & Science*, 16(5), 344-352.
- Han, Seungjin, Lin, Jan T, Yamada, Yasuhiro, & Chung, DDL. (2008). Enhancing the thermal conductivity and compressive modulus of carbon fiber polymer–matrix composites in the through-thickness direction by nanostructuring the interlaminar interface with carbon black. *Carbon*, 46(7), 1060-1071.
- Hashin, Zvi. (1983). Analysis of composite materials—a survey. *Journal of Applied Mechanics*, 50(3), 481-505.

- Heckman, RC. (1973). Finite pulse-time and heat-loss effects in pulse thermal diffusivity measurements. *Journal of Applied Physics*, 44(4), 1455-1460.
- Höhne, Günther, Hemminger, Wolfgang, & Flammersheim, H-J. (2003). *Differential scanning calorimetry*: Springer Science & Business Media.
- Johnston, Andrew A. (1997). *An integrated model of the development of process-induced deformation in autoclave processing of composite structures*. University of British Columbia.
- Kalaprasad, G, Pradeep, P, Mathew, George, Pavithran, C, & Thomas, Sabu. (2000). Thermal conductivity and thermal diffusivity analyses of low-density polyethylene composites reinforced with sisal, glass and intimately mixed sisal/glass fibres. *Composites Science and Technology*, 60(16), 2967-2977.
- Maglić, KD, & Milošević, ND. (2004). Thermal diffusivity measurements of thermographite. *International journal of thermophysics*, 25(1), 237-247.
- NETZSCH. (2008). Operating Instructions DSC 200 F3 Maia. Selb, Germany.
- Osman, Ali. (2015). *Measurement of Multidirectional Thermal Properties of AS4/3501-6 Unidirectional Composite Laminate*. (Master's Thesis), North Carolina A&T State University, Greensboro, North Carolina.
- Parker, WJ, Jenkins, RJ, Butler, CP, & Abbott, GL. (1961). Flash method of determining thermal diffusivity, heat capacity, and thermal conductivity. *Journal of applied physics*, 32(9), 1679-1684.
- Rayleigh, Lord. (1892). LVI. On the influence of obstacles arranged in rectangular order upon the properties of a medium. *The London, Edinburgh, and Dublin Philosophical Magazine and Journal of Science*, 34(211), 481-502.

- Rowe, David Michael. (2005). *Thermoelectrics handbook: macro to nano*: CRC press.
- Saad, Messiha, & Doleman, Bradley. (2013). THERMAL CHARACTERIZATION OF AS4/3501-6 CARBON-EPOXY COMPOSITE. *Frontiers in Heat and Mass Transfer (FHMT)*, 4(2).
- Shim, Hwan-Boh, Seo, Min-Kang, & Park, Soo-Jin. (2002). Thermal conductivity and mechanical properties of various cross-section types carbon fiber-reinforced composites. *Journal of materials science*, 37(9), 1881-1885.
- Springer, George S, & Tsai, Stephen W. (1967). Thermal conductivities of unidirectional materials. *Journal of Composite Materials*, 1(2), 166-173.
- Thornburgh, JD, & Pears, CD. (1965). *Prediction of the thermal conductivity of filled and reinforced plastics*.
- Tian, Tian. (2011). Anisotropic thermal property measurement of carbon-fiber/epoxy composite materials.
- van Laack, Alexander Walter. (2014). *Measurement of Sensory and Cultural Influences on Haptic Quality Perception of Vehicle Interiors*: BoD–Books on Demand.
- Wetherhold, Robert C., & Wang, Jianzhong. (1994). Difficulties in the Theories for Predicting Transverse Thermal Conductivity of Continuous Fiber Composites. *Journal of Composite Materials*, 28(15), 1491-1498. doi: 10.1177/002199839402801507